 CMC, vol.16, no.2, pp.127-173, 2010

Multiscale Modeling of Crystalline Energetic Materials.

O. U. Ojeda[1] **and T. Çağın**[1]

Abstract: The large discrepancy in length and time scales at which characteristic processes of energetic materials are of relevance pose a major challenge for current simulation techniques. We present a systematic study of crystalline energetic materials of different sensitivity and analyze their properties at different theoretical levels. Information like equilibrium structures, vibrational frequencies, conformational rearrangement and mechanical properties like stiffness and elastic properties can be calculated within the density functional theory (DFT) using different levels of approximations. Dynamical properties are obtained by computations using molecular dynamics at finite temperatures through the use of classical force fields. Effect of defects on structure is studied using classical molecular dynamics methods. Temperature induced reactions at elevated temperatures have been studied using ab initio molecular dynamics method for moderate size crystals of nitroethane. Furthermore, while presenting the state of the art in the study of modeling energetic materials, the current advances in the area as well as the limitations of each methodology are discussed.

Keywords: Multi-Scale, Energetic Materials, DFT, MD.

1 Introduction

The need for a multi-scale modeling approach that can probe a material system to provide a description of processes ranging from molecular level to macroscopic behavior is nowhere more obvious than in the study of energetic materials (EM). In order to understand the chemical, physical and mechanical behavior of these materials one needs to employ theories ranging from quantum mechanics/quantum chemistry, molecular dynamics with reactive an non-reactive potentials, statistical thermodynamics, micromechanics, solid mechanics and fluid dynamics allowing for reactions. The energetic materials are stable organic compounds with large negative enthalpies of formation, which are characterized by their ability to undergo chemical transformations starting from the initiation of reactions at the molecular

[1] Texas A&M University, College Station, TX, U.S.A.

level to sustaining a supersonic detonation at macroscopic scale. This multi-scale phenomenon is observed if enough external energy, either in the form of a heat pulse or a large pressure wave, is supplied to a secondary EM so that it reacts, a detonation front will form. In this front, a sudden increase in the material density will be accompanied by a release of temperature, detonation products (usually hot gases), and light, in the opposite direction of the detonation front. This sudden release in pressure and temperature, will effect on the un-reacted mass, ahead of the detonation front, increasing the velocity of its propagation. The time scales and characteristic lengths can vary from a few angstroms, as in the case of lengths of bonds and ordering of molecules within a crystal, to a few nanometers; as in the case of the thickness of initiating reactive layer, and up to a large distance as in the case of the of the material experiencing a shock compression of the expanding wave. The study of effect of the steep changes in density and pressure as the shock propagates through the media if defined through a continuum description requires incorporation of high gradients and rapid variation of field variables (Srivathsa and Ramakrishnan 2008). Although the theory of explosions in gas phase is well developed (Zel'dovich and Raizer 2001; Terao 2007), for a condensed detonating secondary energetic material, which is initiated by another more reactive material, like a metal azide or perchlorates (Campbell, Holland, Malin and Cotter 1956; Volker Weiser 2001) a molecular description is far from being complete (Dlott, Peter and Jane 2003).

In the formulation of plastic bonded explosives, crystals of energetic materials are fragmented and compressed with a binder. In order to describe dynamic response of explosive determination of their mechanical properties is essential, since localization of strain energy has long been the suspect of the formation of reaction zones (Sewell, Menikoff, Bedrov and Smith 2003), or "hot-spots". In addition to this, fracture along a given plane can act as energy barriers and hinder a reaction from completing, hence causing unexpected behavior in some cases.

In the following sections, we aim to present our current effort and relevant results in modeling the complex behavior of energetic materials as well as referring to critical work conducted in this area by other researchers.

We mainly will present a systematic study of crystalline energetic materials and analyze their properties using different levels of theory: at the most fundamental level, we study the ground state properties through the use of the *ab initio* and density functional theory (Kohn and Sham 1965) (DFT) methods. In this study we have used various energetic materials such as cyclotetramethylene tetratintramine (βtHMX), pentaerythritol tetranitrate (PETN), RDX, Fox-7 and nitromethane (NM). We report on structure, electronic structure, and charge densities as a function of applied mechanical stimuli, under volumetric compression, and anisotropic compres-

sion. The structural, mechanical and dynamical properties at finite temperatures are obtained by molecular dynamics simulations with classical atomistic force fields. From these classical simulations various macroscopic properties are extracted. In order to study the reactions in condensed phase we have used ab initio molecular dynamics methods at elevated temperatures. Furthermore, current advances in the area as well as the limitations and failures of each methodology are discussed.

2 Ab Initio Level Modeling of Energetic Materials

Since the earlier studies(Perger, Pandey, Blanco and Zhao 2004); it was clear that a systematic study of the structure and properties of energetic materials was not a simple task that could give meaningful information by the use of a generic basis set. For example, the initial calculated energy barrier for the rearrangement(Dewar and Ritchie 1985) of nitromethane (NM) to methylnitrite (MNT) was 47.0 Kcal/mol. Later, the value of 73.5 Kcal/mol reported by Mckee(McKee 1986) indicated dissociation of NM as the most probable pathway. Nonetheless, Hu's group(Hu, He and Chen Liu, Fan-Chen) reported NM breakdown via C-N bond rupture (61.9 kcal/mol) and Nguyen's group(Nguyen, Le, Hajgato, Veszpremi and Lin 2003) have reported direct dissociation to CH_3 and NO_2 via radical formation (63 kcal/mol). Twenty years later, investigations with a transfer Hamiltonian indicates that the radical formation is the most probable pathway(McClellan, Hughes and Bartlett 2005).

The adiabatic potential energy surface (PES) of the simplest secondary energetic material, NM, shows a multiple energy minima's, caused by the interaction of the nitro oxygen atoms with the methyl hydrogen (Figure 1). We can expect a more complex potential energy surface (PES) for larger and more complex molecules like pentaerythritoltetranitrate (Gruzdkov, Dreger and Gupta 2004) (PETN) and cyclotrimethylenetrinitramine (RDX).

Due to the size and low symmetry of the relevant systems, earlier studies of EM's focused on simple molecules (Miller 1995; Son, Asay, Bdzil and Kober 1995; Soto 1995; Soulard 1995; Tsai 1995; White, Barrett, Mintmire and Elert 1995) and the development of electrostatic potentials(Pinkerton and Martin 1995). The appearance of periodic boundary condition studies came about much later, with the use of the Hartree-Fock approximation and tools like fixed bonds/angles to reduce the degrees of freedom and thus the size of the calculations(Kunz 1995).

We have focused first on developing knowledge at the electronic level within the DFT approximation on the following systems; β-HMX(Cady, Larson and Cromer 1963; Yoo and Cynn 1999; Stevens and Eckhardt 2005), FOX-7 (Gilardi and George 1984; Bemm and Ostmark 1998; Evers, Klapotke, Mayer, Oehlinger and Welch

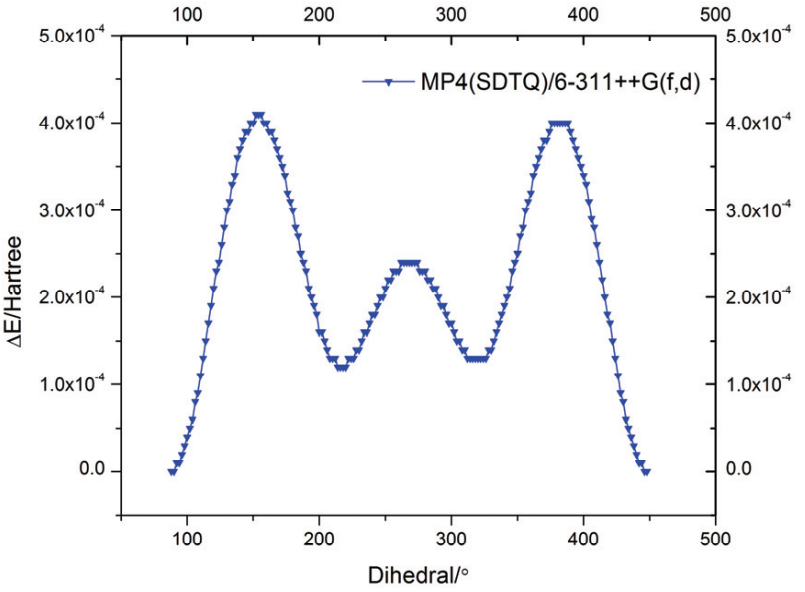

Figure 1: Potential Energy Surface (PES) of NM. The dihedral angle, initially at the optimized position ca. 90° is formed by hydrogen, the central carbon atom and one of the nitro group's oxygen. Increments of 2° used.

2006; Meents, Dittrich, Johnas, Thome and Weckert 2008; Meents, Dittrich, Johnas, Thome and Weckert 2008), TATB(Cady and Larson 1965; John R. Kolb 1979; Bower, Kolb and Pruneda 1980; Lewis L. Stevens 2008), NM(Trevino, Prince and Hubbard 1980; Bagryanskaya and Gatilov 1983; Cromer, Ryan and Schiferl 1985) and PETN-i (Booth and Llewellyn 1947; Olinger, Halleck and Cady 1975; Olinger and Cady 1976; CCSDT 2001).

Energetic materials systems usually have a low symmetry crystal structures. TATB, the system with the lowest symmetry in the unit cell, has a space group P-1, only inversion as the symmetry operation. The higher symmetry system, PETN, is a tetragonal crystal, but its tetrahedral four arm chemical structure, with a sp^3 hybridized central carbon has four resonant nitro groups at the end of these arms, with this stiffer structure, the convergence to small tolerances in both energy (smaller than 3 10^{-6} eV, or 10^{-7} A.U.) of the self-consistent field cycle, and forces (5 10^{-4}eV/A) is required, in ab-initio quantum chemistry calculations.

In the case of plane-wave approximation, we have used both ultra-hard and regular projected-augmented wave method potential lists, with the use of the VASP software. At the above tolerances used, we have found convergence to 700 eV for normal potentials, and 1000 eV for ultra-hard potentials. K-point sampling space converged at a Monkhorst-Pack grid size of 2x2x2. Troullier-Martin pseudopotentials(Troullier and Martins 1991), as well as PAW potentials(Kresse and Hafner 1993; Kresse and Hafner 1994; Kresse and Furthmüller 1996; Kresse and Furthmüller 1996; Kresse and Joubert 1999) for the case of plane wave basis have been used, Further calculations on the systems have been performed with the Crystal06 package using an 6-31G* basis set.

2.1 Equilibrium Properties

Under a specified volume or pressure, the corresponding energy for each system can be describe through the use of a proper equation of state (EOS). We have performed calculations on the crystals of cyclotetramethylene tetratintramine (βtHMX), pentaerythritol tetranitrate (PETN), RDX, FOX-7 and nitromethane (NM), the results are displayed in Figure 2, in order to determine the EOS and equilibrium properties of each.

Studies on the thermochemical properties of β-HMX and its polymorphic phases. (Choi and Boutin 1970; Brill and Goetz 1979; Main 1985), (Pople, von Rague Schleyer, Kaneti and Spitznagel 1988), (Lyman, Liau and Brand 2002) for schemes based on isodesmic (having the same type of bonds) and isogyric (spin-conserved) in which the effect of different basis sets is explored, indicate that a larger 6-311++G(3df,3pd) basis set on geometries optimized with the 6-31G(d) basis set (Cobos 2005) are required. We have performed calculations with the gradient corrected PBE functional (Perdew, Burke and Ernzerhof 1996) on single crystal models using periodic boundary conditions. Extended basis sets(Gatti, Saunders and Roetti 1994) with primitive coefficients for carbon, hydrogen, nitrogen and oxygen, as implemented in the crystal06 package were employed (Dovesi, Saunders, Roetti, Orlando, Zicovich-Wilson, Pascale, Civalleri, Doll, Harrison, Bush, Ph. and Llunell 2007). Initial structures for these crystals were obtained from the Cambridge crystallographic data base (Database 2007). For the case of molecular crystals, the determination of equations of state is the initial step in understanding how different changes in structure can alter the sensitivity of the material (Zeman, S. 2007).

At each state, relaxation of the atomic positions is achieved through optimization of the ionic degrees of freedom; cell shape is optimized through the corresponding cell parameters. The total energies for each system at a given strained volume were used for fitting through the Birch-Murnaghan(Birch 1947) equation of state (Birch

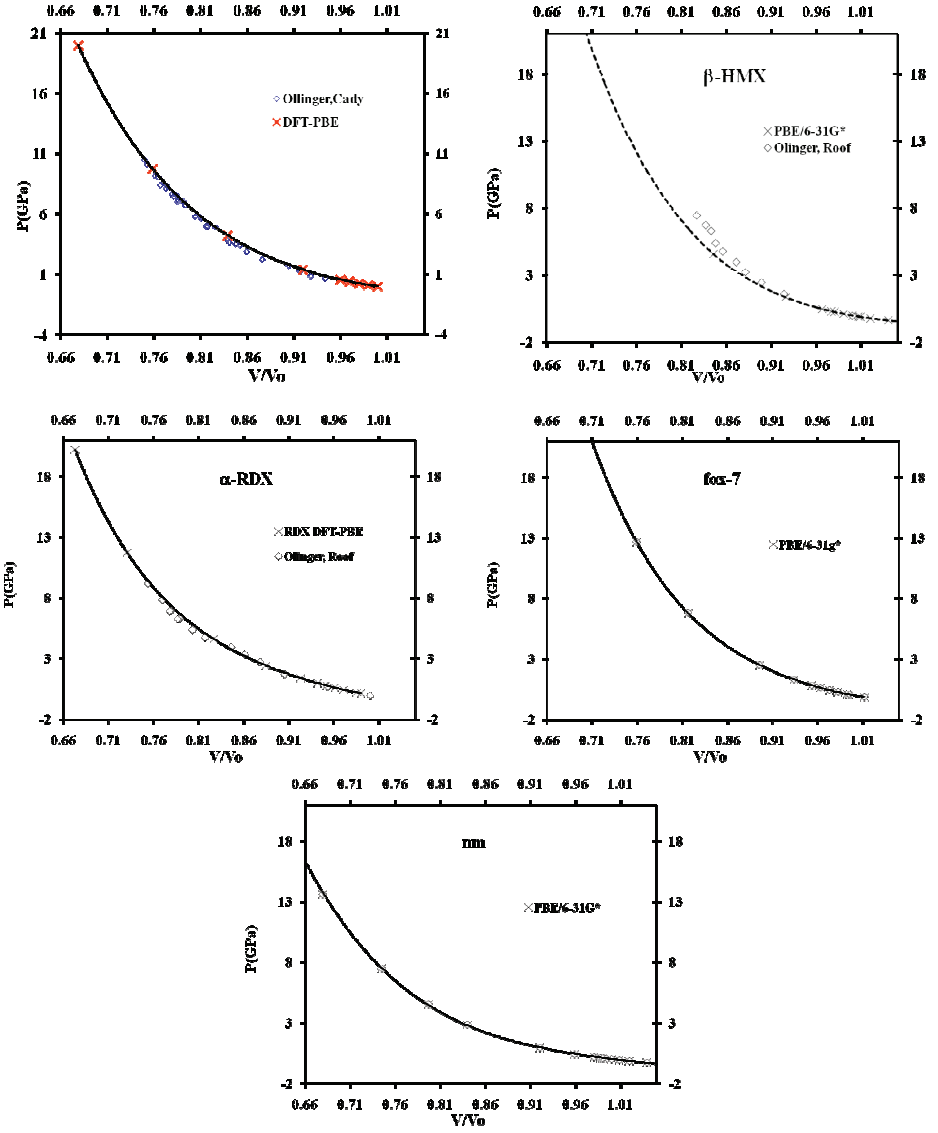

Figure 2: EOS data for PETN, RDX, β-HMX and fox-7; the experimental data (diamond symbols), and the calculated values (squares), using 6-31G*/PBE functionals (squares). In each case, the Birch - Murnaghan EOS fit also shown (solid black lines).

1978) from which one can infer the equilibrium volume, V_o, bulk modulus at zero pressure, B_o, and derivative of bulk modulus, B_o', with respect to pressure. For materials in which cohesive forces in the crystal unit cell are mostly covalent, (as opposed to weaker dispersion forces), usually the equation of state is sufficient to predict phase changes and their relative stability.

It is well known that the impact/shock sensitivity of the EM depend strongly on the geometry of the contact relative to the shape of the sample, the material's structure, morphology and its chemical and thermodynamic properties. Finite linear stress models (i.e., second order elastic constants) may give a best initial approximation to the response of the material under hydrostatic pressures. PETN, which has a tetragonal crystal structure, the optimized volume is found to be 3% higher than the experimental one of 574.638 $Å^3$. Comparison with experimentally observed bulk modulus and equilibrium volumes is summarized in the following table:

Table 1: Equilibrium properties for PETN.

V_o($Å^3$)	B_o(GPa)	B_o'	Reference
600.3	14.5	6.7	(Sewell, Menikoff et al. 2003)
590.8	9.4	11.3	(Olinger, Halleck et al. 1975)
579.47	14.1	10.4	(Sorescu, Rice and Thompson 1999)
595.46	11.26	10.28	This work

Nitromethane, which is a liquid at ambient conditions, has a crystal unit cell of orthorhombic symmetry (No.19). The equilibrium parameters are summarized in Table 2:

Table 2: Equilibrium Parameters for nitromethane

V_o($Å^3$)	B_o(GPa)	B_o'	Reference
310.35	6.78	5.88	(Sorescu, Rice and Thompson 2000)
291.87	9.14	6.10	(Sorescu, Rice et al. 2000)
292.7	7.0	5.7	(Cromer and Schiferl 1985)
290.83	8.22	8.47	This work

The use of larger basis sets, better correlation functions, and an improvement in computational hardware, has made DFT the method of choice of most of the ab-initio calculations reported on energetic materials, which now encompass decomposition mechanisms (Maharrey and Behrens 2005) studies, geometry and electronic structure optimization (Xiao, Ju, Xu and Fang 2004; Ju, Xu and Xiao 2005;

Li, Huang and Dong 2005; Zhang, Shu, Zhao, Dong and Wang 2005), heats of formation (Chen and Wu 2001; Korolev, Petukhova, Pivina, Sheremetev, Miroshnichenko and Ivshin 2004; Qiu, Xiao, Ju and Gong 2005; Byrd and Rice 2006) and models for correlation of sensitivity and heats of detonation (Edwards, Eybl and Johnson 2004; Drake, Hawkins, Hall, Boatz and Brand 2005; Moore, Funk and McGrane 2005; Zhao, Zhang and Li 2005; Badders, Wei, Aldeeb, Rogers and Mannan 2006).

2.2 Electronic Band Structures and Charge Densities

If we let the molecular fragments stand apart at a large distance, while keeping the translational symmetry of the system intact, and perform a SCF calculation, we can obtain the electron density of the non-interacting system. We can determine the difference density map between the electron density of this non-interacting density, and the charge density obtained from the optimized crystal structure of nitromethane. Here, we have used a linear scale, since the difference in the two charge densities is expected to be small. The degree and number of hydrogen bonds can also play a role in the stability and sensitivity of each type of system.

The electronic band-structure, obtained using a 8x8x8 symmetric k-space Monkhorst-Pack integration grid, shown in the following Figure 3 for NM. We have included the Fermi level as a dotted line, to facilitate comparison of the energy levels with the atom projected density of states. To determine the density of states the integration path over the reciprocal space is taken along the high symmetry directions; as displayed in the inset.

The calculated energy band gap at Γ is 1.9E-1 A.U. or 5.24 eV of PETN, Figure 4; which is a characteristic large value for an insulating crystal. There is a larger amount of population coming from oxygen states near the valence band, while the first conduction or exited state band is mostly populated from oxygen and nitrogen states. This indicates the activity the nitrogen and oxygen atoms, which for nitromethane arises only from the nitro groups, in the valence and conduction states.

2.3 Adiabatic Isotropic and Anisotropic Compression of Energetic Materials

If we consider that the first part of a supersonic detonation or shock is always an adiabatic compression of the solid to the Hugoniot line, the behavior of energetic materials through adiabatic compression is of relevance. The effect of compression in the observed temperature has been studied for shocked states (Zel'dovich and Raizer 2001) assuming a vanishing surface upon detonation as:

$$T = T_0 \exp\left(\int_{p_0}^{p} \frac{dP}{\frac{\partial E}{\partial V} + p}\right) \tag{1}$$

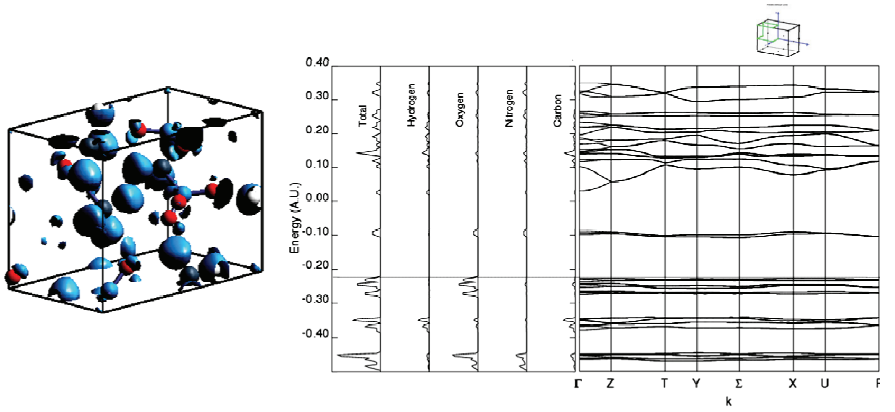

Figure 3: The characteristic large band-gap of these materials can be observed from the electronic band structure (far right), and density of states (center) of Nitromethane. The charge density around each atom is displayed on the left.

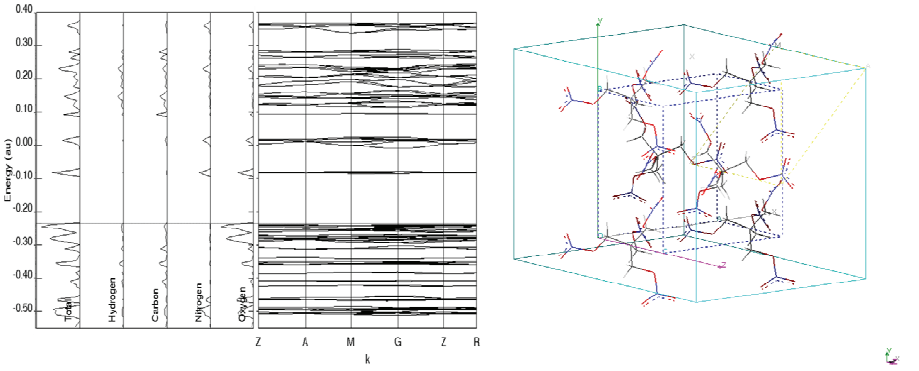

Figure 4: Electronic band structure of PETN. Contribution to the first two available regions above the Fermi energy are due to contributions mostly from oxygen and nitrogen atoms(left). The PETN unit cell (right), the reciprocal space construct is displayed as the outer cube concentric to the primitive cell.

There is an exponential behavior on temperature upon compression. We have studied the uniaxial compression of NM, β-HMX and PETN. Through axial planes and high symmetry family of planes [100], [010], [001], [110], [011], [101] and [111] axes. Prior to each deformation, the system was rotated so the desired plane was oriented along the 'z' axis. We have chosen a somewhat large value of volumetric compression maximum of 30% to understand the behavior that could be encoun-

tered for high-pressure impacts, such as a shock. This value of compression also gave an estimation of each system behavior without compromising the molecular integrity, which constituted each crystal.

Due to symmetry, the compression along [100] and [010] and as well as [101] and [011] directions for PETN are equivalent. This was also observed in the calculated band-structures at different volumetric compression values.

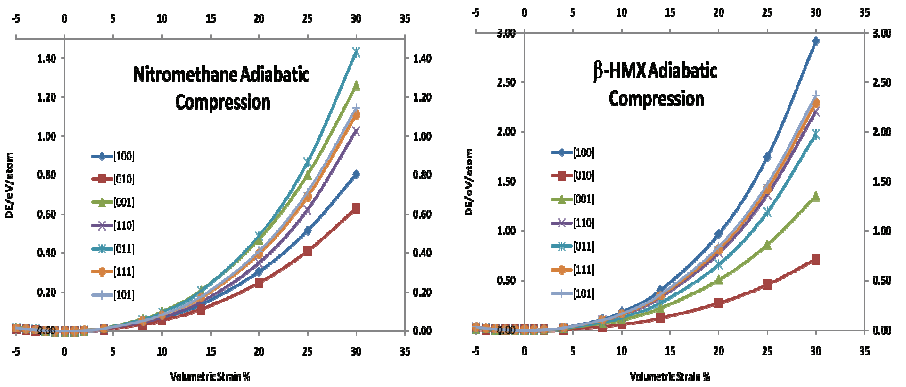

Figure 5: The adiabatic compression behavior of nitromethane (NM) and β-HMX.

From the total change in energy per atom for each system from Figure 5 and Figure 6, we observe that there is a higher energy requirement to attain the compressed state for β-HMX than for the other two systems studied. PETN required a larger energy than NM to be compressed. Uniaxial compression showed the largest change in energy per atom for β-HMX. We can correlate this energy requirement with the trend in sensitivity βtHMX < PETN < NM.

The relationship between an increase in energy that could cause the formation and exited states and anisotropic behavior has been proposed as the cause of anisotropic sensitivity for some systems. We further explore this effect on an adiabatic compression along particular high symmetry planes, for different systems. As the change in energy is correlated with the change in pressure, one would expect there would be substantial change in local temperature along the compression direction with highest energy change.

2.4 Effect of Compression on Electronic Properties: variation of band gap.

The variation of band gap as a function of compression is investigated in these energetic material systems. Figure 7 displays the calculated values of band gap for PETN under hydrostatic compression up to 33%. The variation is non linear in

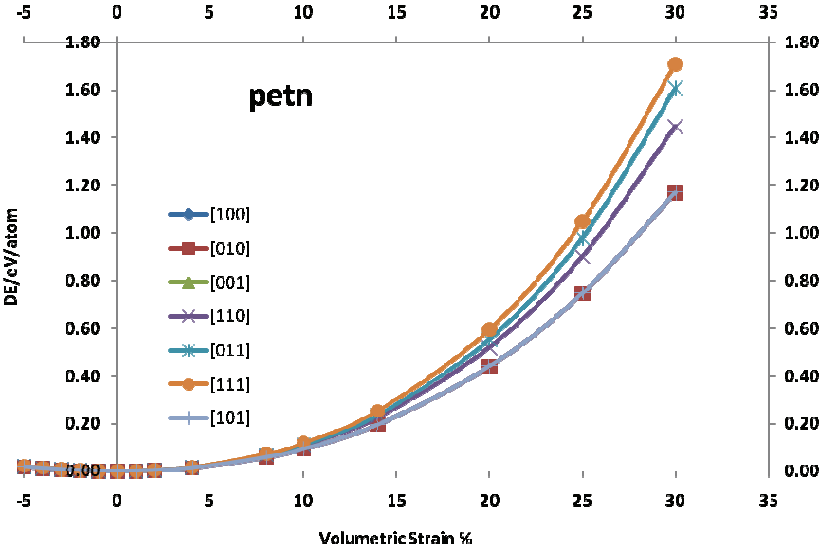

Figure 6: The adiabatic compression of PETN.

volumetric strain. We observe substantial decrease in band gap values, but no band gap closure for the volumetric strain ranges we explored (0% up to 33%).

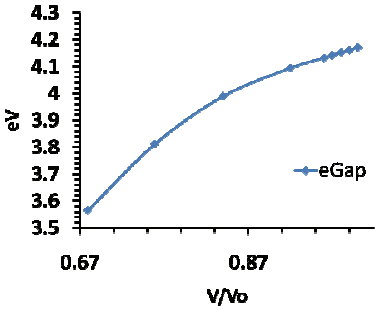

Figure 7: The variation of band gap in PETN under hydrostatic compression.

For PETN and NM, we have calculated the band structure and corresponding band gap along the EOS path. For PETN and NM, we have applied uniaxial compressions along [100], [001], [010], [110], [101], [011] and [111] directions. We observe no band gap closing, even to a value that could be considered to be closed at room temperature (ca. 26 meV) for a hydrostatic compression or for anisotropic

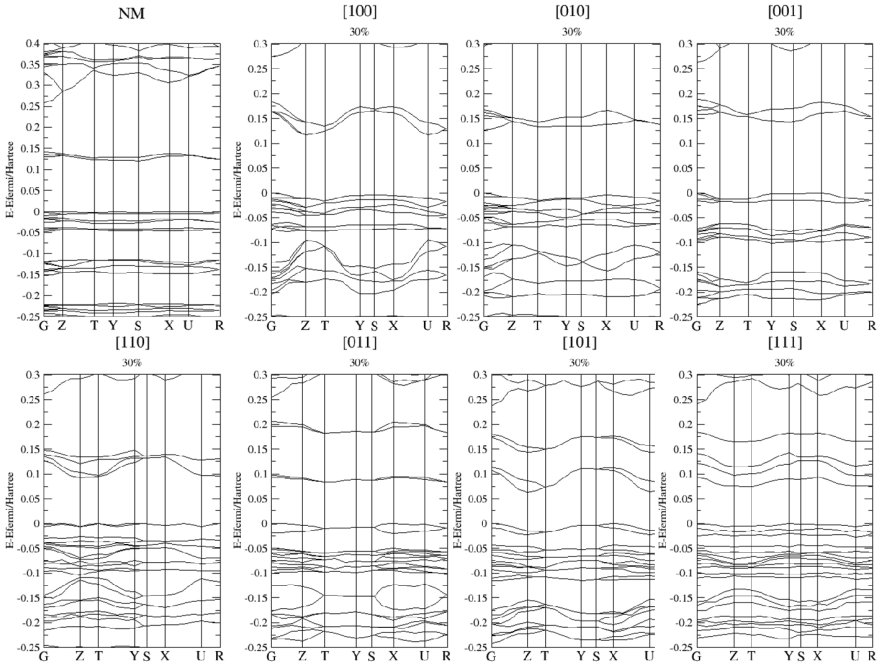

Figure 8: Band structure calculation at the optimized and uniaxially compressed states of NM.

compression. For PETN, we observe almost 2 eV decrease in [111] direction, for NM the decrease is less pronounced even increase is observed in some directions [100], [010] and [001]. The systematic behavior under uniaxial tension is a small but consistent decrease in band gap in all directions tension applied. In order to completely assess the variation of electronic structure as a function of isotropic compression and uniaxial stress one might need to include the effect of defects.

2.5 Vibrational Spectra Analysis of Energetic Materials

Coupling of phonons to low frequency or "doorway" modes have been suggested as an initiation path in energetic materials. In the long range limit, ab initio methods allow for the study of changes with respect to a corresponding pressure via vibrational frequency calculations(Tokmakoff, Fayer and Dlott 1993). We have used the optimized geometries for each system to obtain analytical first derivatives with respect to ionic displacements. Each atom is moved in directions along the three axis by a small step; the energy is then calculated self consistently. A total of 3N+1 calculations should be performed, but this number is reduced when

the symmetries of crystal are taken into account, as it is commonly implemented in the crystal06 code (Pascale, Zicovich-Wilson, López Gejo, Civalleri, Orlando and Dovesi 2004; Zicovich-Wilson, Pascale, Roetti, Saunders, Orlando and Dovesi 2004). The analytical first derivatives are then used to construct the "Hessian" at Γ point through numerical differentiation. The Hessian is the matrix of second derivatives, or force constants that is diagonalized to calculate the mass-weighted dynamical matrix. The number of eigenvalues obtained follows the 3N-6 rule for non-linear molecules, where N is the number of atoms in the molecule and 6 modes correspond to translations and rotations in three dimensions.

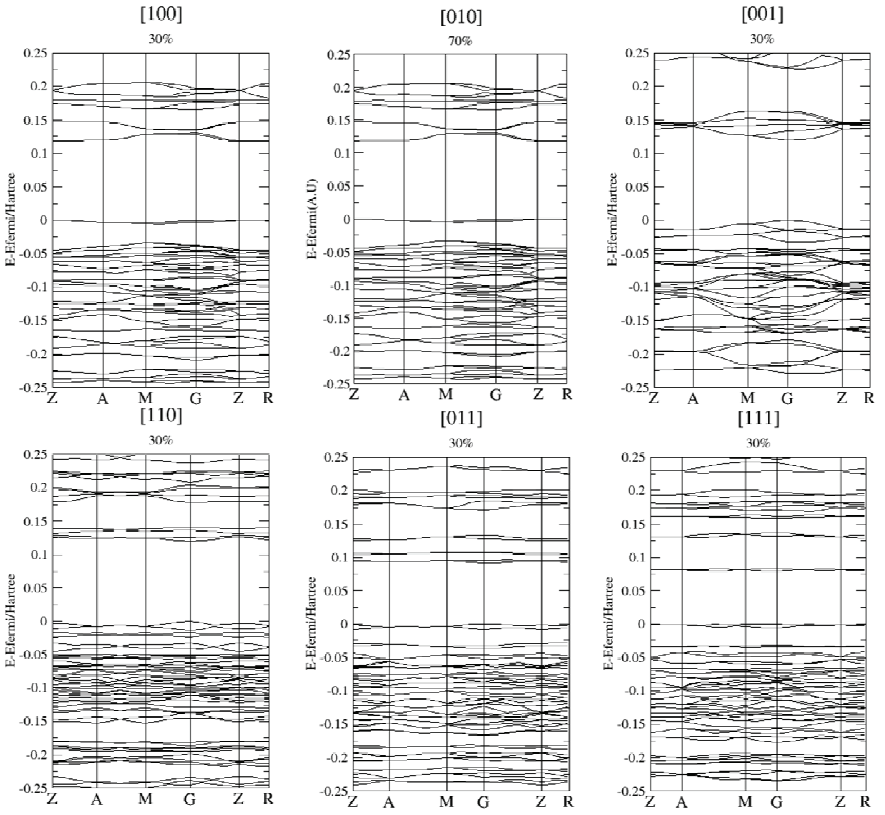

Figure 9: Band structure calculation results at the optimized and under uniaxially compressed states of PETN.

Calculation of the intensities is related to the derivative of the dipole moment with respect to the normal mode coordinate, times its degeneracy. The dipole moment can be obtained from the calculation of the Born effective charges (Zicovich-

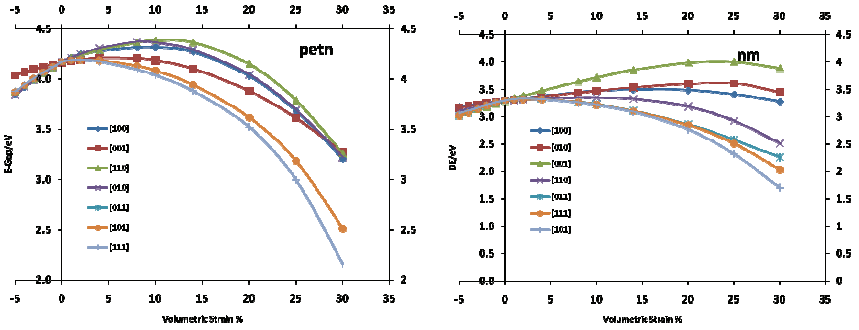

Figure 10: Variation of calculated band gap values of PETN (left) and NM (right) under uniaxial compression conditions.

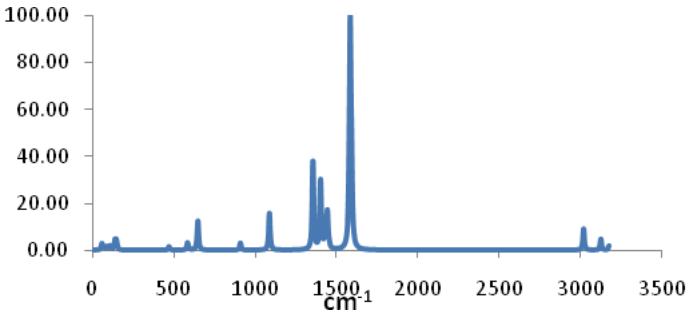

Figure 11: Vibrational spectra of the zero stress structure of NM.

Wilson, Dovesi and Saunders 2001), i.e.; the proportionality constant in the change of polarizability in one direction, with respect to a displacement along another direction.

Large integration grids (XLGRID) and number of K-points (6x6x6 mesh) are required to fulfill the Born charge sum-rule, or the neutrality of the cell. We have further used a tolerance for the differences in the energy for a SCF calculation with a value of 1E-8 A.U. The vibrational spectra, with intensities fitted with the use of Lorentz fits for nitromethane, with a point group C_{2v} (order 4), is displayed Figure 11.

Assignment of each mode has been performed by direct visualization of the eigenvalues(Ugliengo, Viterbo and Chiari 1993; Ugliengo 2006), and from referenced work (McKean and Watt 1976; Ouillon, Pinan-Lucarre, Ranson and Baranovic

2002). The peak, at 650 cm^{-1}, is due to the symmetric NO bending that is accompanied by a C-N stretching, B2-mode. The C-N stretching mode has a frequency of 910 $cm^{-}1$, versus the reported values(McKean and Watt 1976; Ouillon, Pinan-Lucarre et al. 2002) of 917 $cm^{-}1$ and 920 cm^{-1}. Higher in frequency, at 1088, the CH_3 deformation mode (B1) can be found(Ouillon, Pinan-Lucarre et al. 2002). The next peak corresponds to a CH_3 bending mode (δ_2), adjacent to the symmetric NO stretching mode. The maximum at 1441 cm-^{1} corresponds well with the CH_3 bending mode (υ_{10}). The dominant peak at 1548cm^{-1} corresponds the antisymmetric NO stretching mode.

At higher pressures, the relative intensities of low frequency modes (closer to 50 cm^{-1}) increase with respect to the modes close to the largest NO-antisymmetric mode. In general we can see that there is no longer a distinction in from the symmetric NO-stretching from the rest of the deformations with the CH_3 molecule. There are also new peaks appearing in the region from 1432 to 1473. The most predominant peak at pressure of 13.55 GPa is the B1 mode, which is higher in frequency than the other two NO antisymmetric modes (B2, B3), as compared with the 2.89 GPa and 0 GPa states.

At 1432cm^{-1}, the NO-symmetric stretch is accompanied by a deformation of the hydrogen bonds of the methyl group. The symmetric stretch is not so pronounced. We also found that the mode at 1358 cm^{-1} and other modes at lower energies now have non-zero intensities; this would indicate the formation of new bonds or dipole interactions in a regular IR experiment. Also the stretching of the C-N bond, with an oscillation frequency of 975 cm^{-1}, has reduced its intensity to the normalized value of 1.

Table 3: Vibrational and ZPE corrections from vibrational frequencies. Modes at 0 and higher pressures of Nitromethane, frequency values reported in inverse centimeter (cm^{-1}), pressure values reported in GPa, energy in Hartree/unit cell.

		Frequency				Mode	
Pressure	0	2.89	13.55				
	1584	1589	1609		NO	stretching	Anti symmetric
	1443	1437	1473		CH3	bending	
	1402	1410	1432		NO	stretching	Symmetric
	1355	1348	1438		CH3	bending	
	1087	1095	1397		CH3	bending	
	910	926	975		C-N	stretching	
	650	660	686		NO-CN	deform	
ZPE	0.1996	0.2021	0.2086				

The difficulty of assigning fixed position for the hydrogen atoms, led to the conclusion in earlier reports that at ambient conditions the methyl group was able to rotate freely. We can imagine that now that at these high pressures, most likely the methyl group is fixed, due to electrostatic interactions and hydrogen bonding (as indicated by the large increase in the ice peak closer to 3000 cm^{-1}).

Extension along the nitromethane backbone is limited, as indicated by the drastic reduction of the C-N stretch mode. In this way, changes in the structure of the crystal with respect to changes in hydrostatic pressure can be deduced. Changes in conformation and structure can have a direct relationship to properties like elasticity and impact sensitivity.

2.6 Mechanical Properties of Energetic Materials by DFT methods.

It is well known that high energy materials (EM's), for which application ranges from initiators in safety bags, detonation charges, propellants and as secondary explosives, are anisotropically sensitive to heat and mechanical shock (Dick 1984; Dick 1993; Dick 1997). It has been found experimentally, that these materials may undergo detonation by unplanned stimuli. This has raised issues related to transportation cost, safety, logistic and time burdens related to handling of these materials.

For the formulation of plastic bonded explosives, crystals of energetic materials are fragmented and compressed with a binder. Understanding the mechanical properties is required, since localization of strain energy has long been the suspect of the formation of reaction zones (Sewell, Menikoff et al. 2003), or "hot-spots". In addition to this, fractures along a given plane can act as energy barriers and hinder a complete reaction, causing unexpected behavior in some cases. When the applied mechanic shear exceeds the strength of the lattice, plastic deformation arises and multiple dislocations, growth of defects can occur. Therefore the knowledge of the elastic properties is crucial in understanding the material's initial response.

We have performed calculations on the crystals of (βtHMX), NM, RDX, TATB, Fox-7 and PETN using CRYSTAL program. In our earlier work we have studied anisotropic elasticity of various metals, ceramics and oxides using mainly plane wave approaches (Uludogan, Çağın, 2006; Uludogan, Guarin, Gomez, Çağın, Goddard, 2008; Kart, Uludogan, Karaman, Çağın, 2008; Bilge, Kart, Kart, Çağın 2008; Chakrabarty, Çağın, 2008; Kalay, Kart, Kart, Çağın, 2009; Sevik, Çağın, 2009; Pham, Çağın, 2010).

By applying small strains to the crystallographic unit cell, a change from the original, optimized cell energy is obtained. This difference in energy can then be com-

pared in terms of polynomial expansion, to the strain energy;

$$E_0 - E = V_o C_i \eta_j + \frac{V_o}{2} C_{ij} \eta_i \eta_j + \tag{2}$$

Where V_o is the initial "un-deformed" cell volume, and η_i and η_j are the applied elastic Cauchy or "engineering" type of strains. Since we are interested only on the symmetric part of the strain tensor, we can employ the contracted or "Voigt" notation. C_{ij} are then the second order elastic constants.

$$C_{ij} = \frac{1}{V_0} \frac{\partial^2 E}{\partial \eta_i \partial \eta_j} \tag{3}$$

If we realize that the initial reference cell is subject to no additional forces, this is, in its "zero stress" state, the first term in the expansions is ignored. Comparison to a second or higher order polynomial fit against a strain-energy curve will enable us to obtain the corresponding second order elastic constants. The resulting second and higher order elastic constants can in turn be related to the anisotropic response of the crystal to mechanical stimuli. Due to the ample experimental data available(Winey and Gupta 2001; Sun, Winey, Hemmi, Dreger, Zimmerman, Gupta, Torchinsky and Nelson 2008), elastic constant values of PETN allow for a direct assessment of the accuracy of the calculation. A summary is found in the following table.

Table 4: Second order elastic constants of PETN. Comparison is made with experimental data, values in GPa. Value of the calculated Bo from the equation of state.

	6-31G*/PBE	Exp (Sun, Winey et al. 2008)	Exp (Winey and Gupta 2001)
C_{11}	17.88	17.12	17.22
C_{12}	8.10	6.06	5.44
C_{33}	13.44	12.18	12.17
C_{13}	10.17	7.98	7.99
C_{44}	5.42	5.03	5.04
C_{66}	2.95	3.81	3.95
B_o	11.79	10.05	9.94
V	592.73	574.64	574.64

For the case of PETN, we have studied the full elastic tensor at different applied pressures. Stability conditions for this tetragonal system are;

$$C_{11} - C_{12} > 0 \tag{4}$$

$$C_{11}+C_{12}+C_{33}>0 \tag{5}$$

$$(C_{11}+C_{12})C_{33}-2C_{13}^2>0 \tag{6}$$

$$C_{44}>0 \tag{7}$$

$$C_{66}>0 \tag{8}$$

The last two conditions are fulfilled clearly for all the applied pressures. This applies for the second condition two, as none of the involved constants takes a negative value. The rest of the conditions at the studied pressure values are summarized in the following table:

Table 5: Mechanical Stability Conditions for PETN.

P	c_{11}-c_{12}	$(C_{11}+C_{12})C_{33}$-$2C_{13}^2$
0.00	9.78	142.35
0.12	10.90	161.44
0.25	12.27	176.68
0.41	13.58	198.24
1.39	21.46	414.79
4.25	41.54	1334.39

For crystal of other symmetries, no instabilities were found.

The value of the elastic constants can provide an insight into the anisotropic strength of the intermolecular interactions. Although there are other various reports that try to relate Cauchy strains with respect to pressure with the value of the elastic constants, we can only take the values as approximate, as the methodology of obtaining them is rather indirect. For example, Brand attempted to obtain the first three elastic constants(Brand 2006) with a STO-3G basis sets and Hartree Fock approximation, but the elastic constants were obtained from stress/strain curves, along each crystal vector (only 3 constants total). For the case of NM, although no available data on the elastic constants was available, the predicted higher sensitivity along the [001] direction, as predicted by the model of steric hindrance, is supported by the lowest value of this constant predicted in our study

Our calculated values for PETN agrees with the calculated by Gupta's group with sound speed experiments(Winey and Gupta 2001). Values of the bulk modulus and its pressure derivative correspond well to the ones found experimentally by Ollinger, Halleck and Cady, (Olinger, Halleck et al. 1975). The trend $C_{11}<C_{33}$ for this system is an indication of the increased sensitivity found along the [110] plane. For β-HMX there has been evidence(Palmer and Field 1982) of a cleavage

Table 6: Calculated elastic constants of Energetic Materials. For the systems, NM and b-HMX, this represents the full elasticity tensor. Only the diagonal terms are reported for the remaining systems. The values are in GPa.

	NM	$\beta-$HMX	Fox-7	RDX	TATB
C_{11}	17.38	19.00	37.56	79.66	23.62
C_{22}	11.98	17.66	19.79	18.23	76.55
C_{33}	11.92	17.88	46.60	17.40	15.00
C_{44}	5.02	10.65			
C_{55}	3.44	6.01			
C_{66}	4.91	8.51			
C_{12}	6.42	10.7			
C_{13}	9.19	9.93			
C_{15}	-	-0.22			
C_{23}	7.13	11.81			
C_{25}	-	-3.72			
C_{35}	-	-2.01			
C_{46}	-	-3.83			

plane along the (011) plane, is further supported by the observation of a weaker C_{11} constants as compared to C_{22} and C_{33}. Calculated values for bulk modulus and pressure derivatives are in good agreement with experimental observations(Stevens and Eckhardt 2005).

2.7 Empirical Van der Waals correction to DFT energies.

Despite its successful application in many strongly bound systems, current approximations employed within Density Functional Theory(Kohn and Sham 1965) (DFT) methodologies have been unable to correctly predict interactions that are significant to various biological and biochemical molecules (Grimme, Antony, Schwabe and Muck-Lichtenfeld 2007) and neutral molecule crystals like those of rare-gas dimmers(Tsuzuki and Luthi 2001; Tao and Perdew 2005), polycyclic and aromatic hydrocarbons(Suzuki, Green, Bumgarner, Dasgupta, Goddard and Blake 1992; Goursot, Mineva, Kevorkyants and Talbi 2007), and energetic materials (Olinger, Halleck et al. 1975; Hemmi, Dreger, Gruzdkov, Winey and Gupta 2006; Byrd and Rice 2007) (EM). Besides being a requirement for developing engineering models and to understand the behavior of the material in the conditions of its envisioned applications, a proper description of the potential energy surface bears further implications when determining thermodynamic properties like bulk modulus, and second and higher order elastic constants.

It has been suggested in literature that the lack of a proper description of the equilibrium volumes in these molecular systems (Blöchl 1994; Kresse and Joubert 1999; Wu, Vargas, Nayak, Lotrich and Scoles 2001; Kurita, Inoue and Sekino 2003; Stefan 2004; Chakarova and Schroder 2005; Thonhauser, Cooper, Shen, Puzder, Hyldgaard and Langreth 2007) can be attributed to the lack of a proper description of the long range induced dipoles by neighboring molecules. To overcome this hurdle, some recent efforts have been directed towards developing methodologies to specific type of systems, like polymers (Kleis and Schroder 2005) or rare-gas dimers. Some attempts to improve current description of intermolecular forces at a higher level of theory include the choosing of a better description of the exchange functional, with some success mostly from parameterized generalized gradient approximations (Tao and Perdew 2005) and other hybrid functionals, i.e.; X3LYP (Xu and Goddard 2004), the use of orbital-dependent functionals(Engel 2003), optimized effective potentials (Qin Wu and Weitao 2003) or the addition of an external correction to the total ground state energy (Gonzalez and Lim 2003; Stefan 2004; Ortmann, Bechstedt and Schmidt 2006). Perturbation methods, like the spin-component-scaled MP2, have been estimated as inadequate for common pi-stacking and hydrogen bonded interactions (Bachorz, Bischoff, Hofener, Klopper, Ottiger, Leist, Frey and Leutwyler 2008).

We have decided to test the idea of correcting the total energy of the equations of state for NM and PETN, by introducing a damped Buckingham type of potential (Hepburn, Scoles and Penco 1975; LeSar 1984) that accounts for dispersion forces. The implemented empirical term for the dispersion energy was developed by Elstner and Le Sar (LeSar 1984; Marcus, Pavel, Thomas, Sandor and Efthimios 2001):

$$E_{vdW} = \sum_{ij} \frac{c_6^{\alpha\beta}}{R_{ij}^{\alpha\beta 6}} f(R) \tag{9}$$

The damping function used here allows a decay to zero at a value ca. 3 Angstrom, to avoid over counting of energy due to bonding. For ease of comparison, the inner and outer exponents are constantly kept as 7 and 4, to allow for a similar behavior of the decay distance as previously reported results. The parameter "d", called the decay factor, is related to the value at which the damped function will experience an inflexion (viz. $1/r^6$), a value of 3 is chosen for the present calculations. The form of the functional is important since evaluation of fist and higher order derivatives (e.g.; gradients, polarization, etc...) is necessary for calculation of other system properties. In this way, correction of the total energy determined from the Kohn-Sham Hamiltonian is corrected with the addition of an E_{vdw} term:

$$E_{total} = E_{KS} + E_{vdw} \tag{10}$$

Using polarizability values obtained at the MP2 level, Williams and Malhorta(Williams and Malhotra 2006) have obtained C6 coefficients that can be used in calculations with the 6-21G(**) basis sets used to reproduced the energetic behavior of 24 hydrogen bonding and Van der Waals molecular interaction. These were obtained from scaling DFT energies to values calculated at the MP2/cc-pVQZ level, for dimmers like ethane, formaldehyde, benzene, water, etc.

For PETN, in which 2 type of oxygen atoms, one bridging and a pair sharing a resonant bond in the nitro group are present, two different coefficients for nitrogen have been utilized. For those interactions whose coefficients were not reported, Van der Waals radii and coefficients have been obtained as described previously(Williams and Malhotra 2006), based on hybridization or chemical environment of the atomic species. We have followed the same nomenclature used by Miller, e.g.; a tetrahedral sp^3 carbon is labeled (CTE), a sp^3-hybridized oxygen is named OTE and so forth. By means of atomic polarizability values (p_α), coefficients can then be scaled using also the number of effective electrons, with a methodology proposed by Halgreen. (Halgren 1992),The C6 coefficient is then obtained by means of the Slater-Kirkwood approximation (Slater and Kirkwood 1931):

$$C_6^{\alpha\beta} = \frac{2C_6^{\alpha}C_6^{\beta}p_\alpha p_\beta}{C_6^{\alpha}p_\alpha^2 + C_6^{\beta}p_\beta^2} \tag{11}$$

Since R^{-6} interactions should dominate at long enough distances (Alonso and Mañanes 2007), we have considered summation of the E_{vdw} interactions not in one, but in a super-cell considering 4x4x4 primitive cells. Equilibrium parameters have been additionally been obtained for the systems: m-dinitrobenzene(Trotter and Williston 1966; Wojcik, Mossakowska, Holband and Bartkowiak 2002), 2-4-6-trinitrotoluene (Coleburn and T. P. Liddiard 1966; Coleburn 1970; Golovina, Titkov, Raevskii and Atovmyan 1994; Stevens, Velisavljevic, Hooks and Dattelbaum 2008), ethanol (Brown, Slutsky, Nelson and Cheng 1988), benzene (Cox 1958; Bacon, Curry and Wilson 1964; Jeffrey, Ruble, McMullan and Pople 1987), urea (Fischer and Zarembow 1970; Swaminathan, Craven and McMullan 1984; Haussuhl 2001), cyclohexa-2,5-diene-1,4-dione (Boldyreva 2003) (p-quinone), Benzene-1,3-diol (resorcinol) (Day, Price and Leslie 2001), g-glycine (Boldyreva 2008).

There is a drastic effect on the results obtained from VdW as opposed to neglect of dispersion. Although the difference in the bulk modulus is still bigger than 18%, the small discrepancy (below 5%) between the predicted equilibrium volume and the one used for reference in the initial calculations, indicates that an empirical correction can be further refined to yield values closer to experimental ones, without sacrificing computational time.

Table 7: Effect of VdW correction to DFT energies in the calculation of elastic constants. Values are in GPa. Volume in A^3

	C11	C33	C22	V
PETN-NOV	17.67	5.51	-	696.05
PETN-VDW	33.32	11.90	-	609.84
PETN-EXP	23.11	17.35	-	574.64
NM-NOV	58.68	5.25	2.36	254.11
NM-VDW	71.92	9.42	6.06	297.19
Resorcinol-VdW	26.68	57.23	41.96	490.61
Resorcinol-exp	8.60	19.50	28.80	534.70

3 Classical Force Field Based Simulations

Models like the Hugoniot equation have been applied to the processing of energetic materials(Firsich 1984; Sun, Garimella, Singh and Naik 2005), and the effect of detonation in pressure shock-waves has been investigated (Novozhilov 2005; Patterson, Lagutchev, Hambir, Huang, Yu and Dlott 2005; Urtiew and Tarver 2005). To this regard, constitutive relationships, like isotherms and isobars, can be obtained for the unreacted crystal by means of molecular dynamics methods. We have performed molecular mechanics and molecular dynamics calculations with the DREIDING force fields (Mayo, Olafson and Goddard 1988) as well as the following force fields; CVFF (Hagler, Huler and Lifson 1974; Hagler and Lifson 1974; Hagler, Dauber and Lifson 1979; Hagler, Lifson and Dauber 1979; Lifson, Hagler and Dauber 1979; Kitson and Hagler 1988; Kitson and Hagler 1988; Pnina Dauber-Osguthorpe 1988), Compass (David Rigby 1997; Sun and Rigby 1997; Sun 1998; Sun, Ren and Fried 1998) and Universal (Rappe, Casewit, Colwell, Goddard and Skiff 1992).

Whenever the force field assigned atomic charges were not available (i.e. Universal, DREIDING), a charge equilibration method: the QEq method (Rappe and Goddard 1991) employed for charge assignments. For these simulations, with the Isothermal Isobaric ensemble (NPT) the code LAMMPS (Plimpton 1995), Cerius2 and Materials Studio have been used. Multiple in-house scripts and codes have been developed to analyze and perform data analysis.

We have found that for the pressures closer to ambient conditions, NM will have the largest thermal expansion.

In common applications, compression of EM's with a polymeric binder facilitates casting and machining. This is usually done with a small weight percent of binder included in the formulation. For example, composition LX-16 has 96%w PETN

and the rest as polymer binder (1980). Heterogeneities in the microstructure of polymer-bonded explosives raise difficulties in understanding trends like sensitivity and mechanical properties, as compared to the homogeneous material. Unlike other systems, e.g.; metals, the effect of plasticity in detonation properties of energetic materials remains a nascent topic; processing parameters can have an effect in the sensitivity of the energetic materials. Crystals purified with different solvents, e.g.; cyclohexanone or acetone, will produce different number of cavities and voids (Lionel Borne 1999), and become sources of dislocations. Changing from cyclohexanol/ethanol to γ-butyrolactone/water change the crystallization morphology of RDX from small crystallites to dendrites (Antoine E. D. M. van der Heijden 2008). The effect of the void and vacancy concentration has been suggested to have an effect in the sensitivity of systems like RDX and HMX (Ruth M. Doherty 2008). Crystallization conditions will also have an effect on the specific morphology of the grown crystal habit (Zepeda-Ruiz, Maiti, Gee, Gilmer and Weeks 2006).

Understanding the thermodynamic and elastic effects in sensitivity can help tailor some of the applications of EM's to the civilian realms..(Lozano and Fernandez 2007), and also reduce associated hazard of transporting and handling of the materials. The prepared crystals are usually compressed to achieve high density either with other type of energetic materials, or with a plastic binder. Detonation pressure for a given system will depend (Hartmut Kröber 2008) on the density of the material; therefore, compression to achieve high density in this binder-energetic material matrix is performed. Since there is a small weight percent of plastic binder, stresses localization caused by the close contact of different crystal faces can be expected, specially under conditions of high stress rate (as in direct impacts) or supersonic shock strains.

3.1 Effects of Defects in Energetic Materials.

It has already been shown that defects have an effect on the sensitivity to impact of the energetic materials. We want to explore the effect of crystal defects on the anisotropic mechanical response of the energetic materials under both hydrostatic and axial compression, and with the application of shock. It has been suggested that grain size and orientation more than void concentration can have an effect on the detonation pressure of some energetic materials (Czerski and Proud 2007; Landerville, Oleynik and White 2009). By means of molecular dynamics simulations, we show the results of the studies on a commonly used secondary explosive; PETN, which has an anisotropic response to shock detonation. The goal is to understand the role of deformation mechanisms in the initiation of the energetic materials.

The slip plane has been suggested as the (110) plane, with possible Burgers vectors in <111> (Gallagher, Halfpenny, Miller, Sherwood and Tabor 1992), other studies

suggest the formation of a slip system in [110](001) (Dick 1984). By means of layer projection, we have created large super cells (up to 868 molecules) of the latter, and studied by means of molecular mechanics and molecular dynamics simulations. Creation of the [110]- and [001]- layers with 3-D periodic boundary condition was performed initially on the single crystal system. This layers were then expanded to a matching length of ca. 35 A per side. Stacking along the z-axis of the [001] was used for alignment. This created the first set of bi-crystals for simulation. After the results of molecular dynamics simulations were obtained, a larger grain system was set up. In this case the z-direction was doubled in size, with the intention of reducing the finite size effects of the stacking fault in the grain system. The crystal packing of PETN facilitates identification of a discrete number of layers on each side of the grain system.

In order to assess the quality of the force fields, molecular dynamics simulations have been performed in a large (4x4x6) super cell of PETN. The initial applied temperature (50K) was ramped in increments of 50K up to a value of 550K. Averages were obtained for the last 40 ps from the 60 ps run. Equilibrium volumes at 300K (621 $Å^3$) are comparable to the experimental reported values(Booth and Llewellyn 1947).

From these runs initial structures of obtained for the succeeding molecular dynamics simulations to obtain the relaxed system's energies, at 50, 250 and 300K. The initial 50K temperature is employed in order increase the temperature gradually of the system to the target value of 300K. There is already a change in the density of the material when prepared along one phase, as compared to the denser packing found in the [110] direction. There is a stacking fault caused by the atom mismatch in the inter-planar spacing of the [110] direction as compared to the [100] direction.

The surface energy is calculated using the following formula:

$$\Delta E = E_1 - nE_0 \tag{12}$$

Here E_1 indicates the grain system energy, E_o the minimum energy per face (Eo/2) and n is the number of molecules in the system.

From molecular mechanics calculations, which were iterated up to 2000 steps, with a convergence on the energy of 10^{-3} Kcal/mol and a convergence on the forces of 0.5 Kcal/mol/Å, we are able to obtain the energetic of the formation of the system. The first set of results can be observed in the following figure.

Molecular Dynamics Simulations show also a positive energy of formation for the interface. In here, we have been able to construct a thicker bi-crystal. We can see a change in the energy profile close to 9. Closer inspection of the structures shows a change in the crystal orientation, caused by the plane mismatch. We see also a

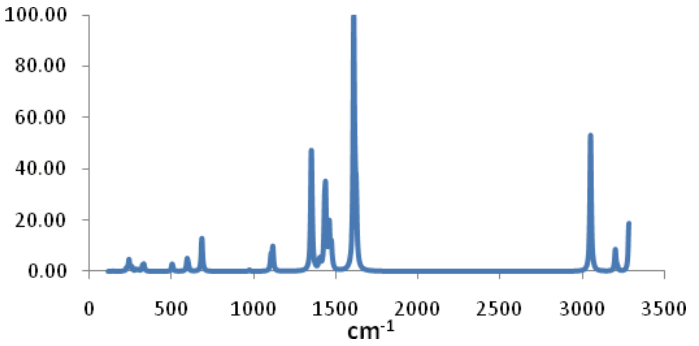

Figure 12: Vibrational spectra of NM, (IR region), corresponding pressure of 13.55 GPa.

reduction in the total energy with respect of temperature.

At the interface, there seems to be a larger number density of nitro groups expanding from the [110] crystal, this could explain the increased reactivity observed for compressions along this direction. Formation of the grain system shows an initial change in the density of material, although the density increases to with the number of layers, it is not expected to reach the value of the defect free system.

After the initial observation of the effect of crystal orientation and sensitivity found in PETN by Dick(Dick 1984), a model of steric hindrance was put forward. In this model, it is assumed that sensitivity will be related to the number of intermolecular close contacts that can be found when straining along a particular direction. Based on surface etchings, Sherwood (Gallagher, Halfpenny et al. 1992) has reported a Burgers vector as b<1,-1,1> and a length of 1.48 nm. Their study has concluded that for the suggested slip system, steric hindrance would be limited to half as the one observed in our studied system; Although both in the early reports by Dick and Sherwood, acknowledge is made to the high number of intermolecular contacts is made in the (110)(001) grain system, no further discussion is presented. Our simulations indicate that possible smaller Burgers vector can be realized for this type of grain.

4 Ab initio Molecular Dynamics Simulations

The specific properties of high performance and sensitivity have to be considered for stable energetic materials. Higher risk efforts are underway to explore the possibility of meta-stable energetic materials. There has been extensive research to measure the kinetics and elucidate the mechanism of their decomposition for a long

time. The study of thermal decomposition mechanism is essential to engineering design and fundamental to the design and optimization of materials. The kinetics of thermal decomposition is expected to illustrate the mechanisms of initiation and stability. In this section, we will focus on the decomposition pathways in gas-phase and investigate their thermodynamic properties in condense phase, from molecular dynamics simulations within a 'first principles' methodology.

C–NO_2 bond rupture is often suggested as an initial step in the thermal decomposition of nitro compounds, because the attachment of nitro groups is relatively weak(Manaa and Fried 1998; Manaa, Reed, Fried and Goldman 2009). The C–N bond dissociates without an apparent transition state structure, and affords two radicals. The calculated reaction enthalpy for gas-phase nitroethane to form radicals is 56.1 kcal/mol at the B3LYP/6-31+G(d) level. To better understand the C–NO_2 bond rupture, a detailed reaction profile was calculated as a function of C–NO_2 bond length.

The converged (10^{-7} atomic units (au)) wavefunctions from the initial position were used as initial guess for the first Car-Parrinello molecular dynamics run. Since the initial gradients can be very large, an initial kinetic energy of 50K was used. Atoms were allowed to move, and then the kinetic energy was slowly removed. From this "annealing" procedure an equilibrium configuration of the electron density and ionic positions was obtained. The electronic density for each atom was used for the Parrinello-Rahman microcanonical ensemble simulations that followed the damping run.

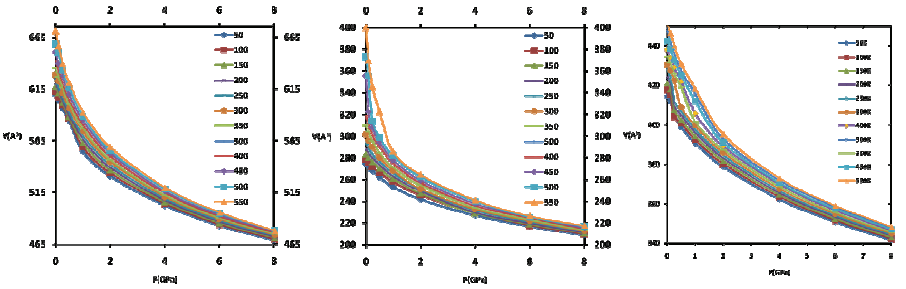

Figure 13: Isotherms for PETN(left), NM(centre), and TATB (right)

An initial equilibration run of 2000 steps, with a step size of 4 au (1 au= 0.024188843 femtoseconds). Then a longer run of 2000 steps, with velocity scaling of 200 K was realized, All at 50K and doubled initial temperature. We see from the instantaneous values (Figure 19) that the system is closer to its equilibrium configuration. The

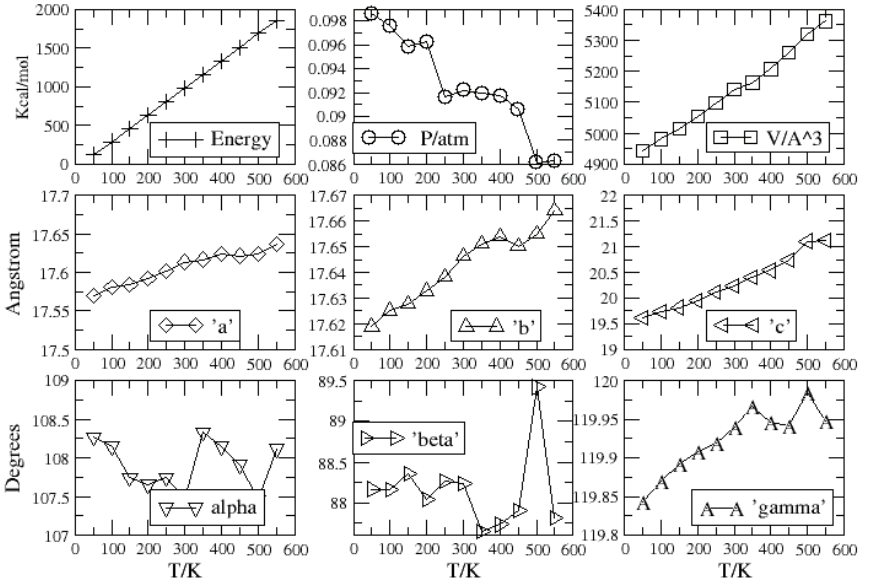

Figure 14: Structure Parameters of TATB at different pressures.

conserved energy (E-con) is in fact stable ca. -225.1261 Hartree. From these simulations we can extract the average value of the electronic (fictitious) kinetic energy, and use as input for constant temperature simulations, with Nose thermostats for the ions and the electrons. This simulation can further be used to obtain equilibrium values and averages at higher temperatures. An upper limit of 300K is proposed, with increments of 50K and averages of 80000 steps.

At the detonation transition, the temperature of NM has been estimated(Bouyer, Darbord, Hervé, Baudin, Le Gallic, Clément and Chavent 2006) as 2500K Temperatures in excess of 10^4 K have been found (Tarasov, Karpenko, Sudovtsov and Tolshmyakov 2007) in compressed air inside detonating PETN.

After the equilibrium volumes were found, a larger Nitroethane cell was constructed, with an approximate density of that of the liquid ($1g/cm^3$). Here again the challenge was first to obtain an appropriate wavefunction to be used in calculations at higher temperatures. The obtained wavefunction was used as input to perform car-parrinello molecular dynamics at constant volume and energy. This procedure applied to explore determining any or which chemical reactions occurring at a given elevated temperature.

From the different snapshots taken at this initial step, we see even at the lower

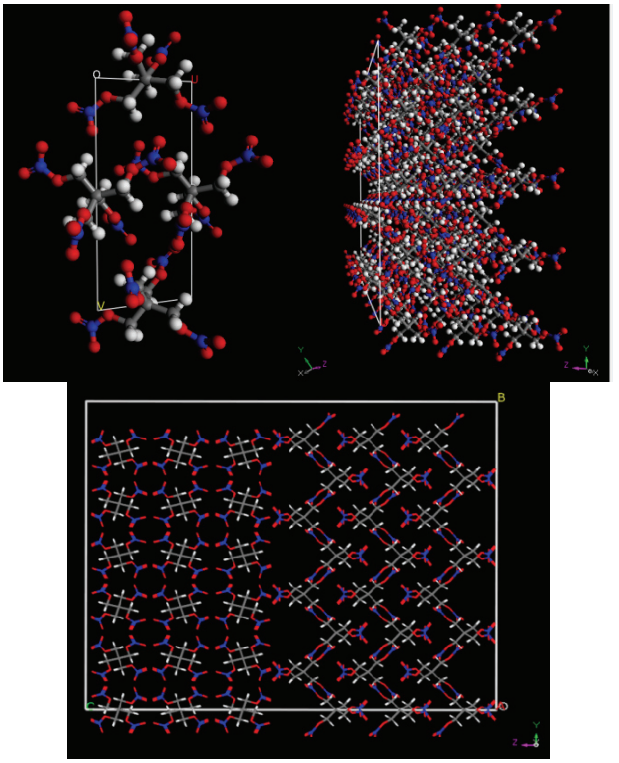

Figure 15: [110] plane (TOP) and [001] layer of PETN. Bottom: [110][001] Grain boundary system of PETN

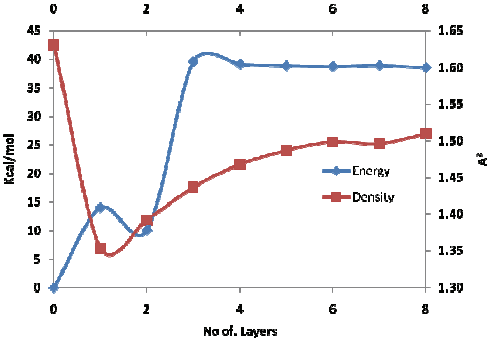

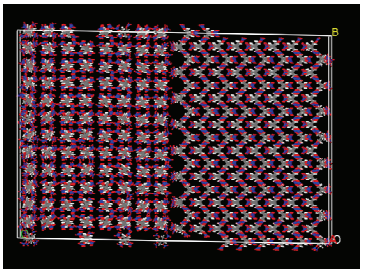

Figure 16: Change in energy and density with respect of number of layers (left), 8 layers system observed from the [001] direction.(right)

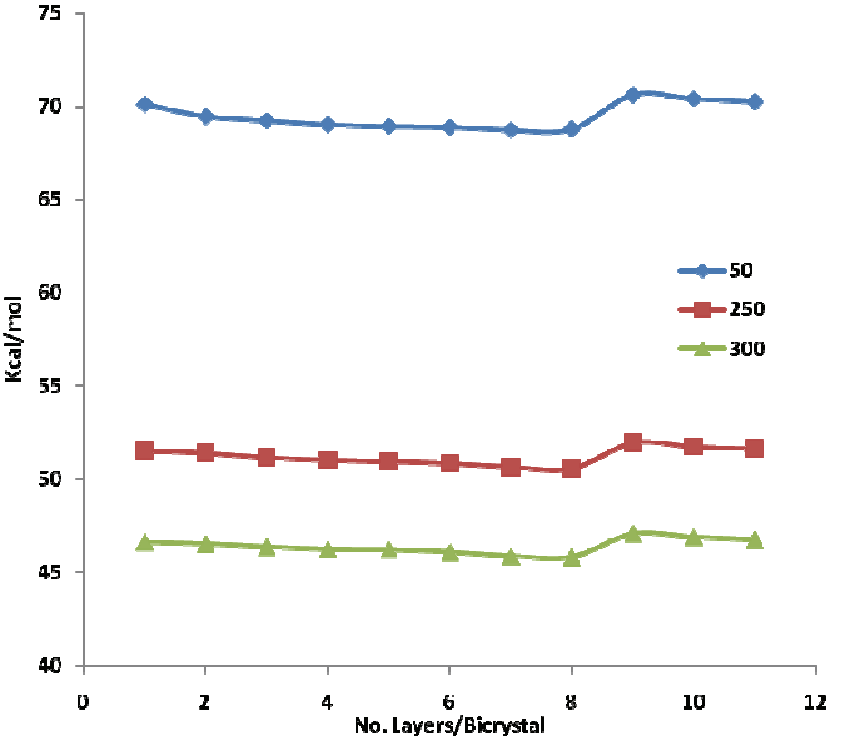

Figure 17: Change in Energy with respect to bi-crystal thickness

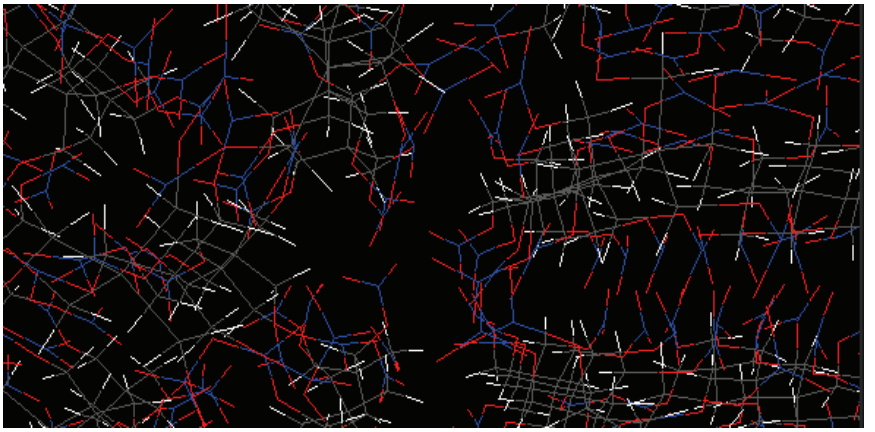

Figure 18: Interface at the [001] direction (LEFT) and the [110] plane(RIGHT), snapshot from the MD simulation at 250K. Oxygen atoms represented in red, nitrogen in blue and carbon as gray (hydrogen is white)

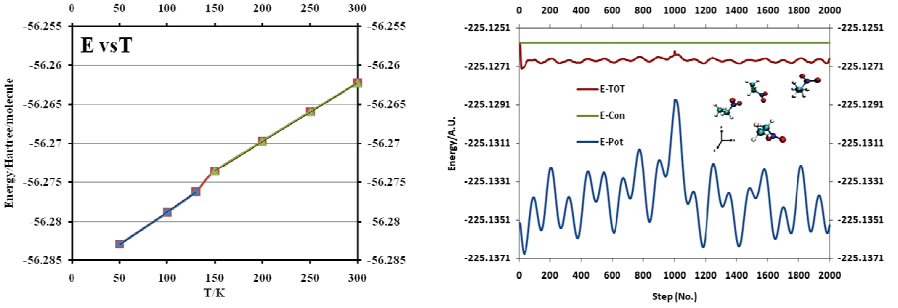

Figure 19: Internal energy of NE as a function of temperature (LEFT); Instantaneous values for the components of energy for 2000 steps of MD simulation of Nitroethane.

temperature of 1000 K, that the initial bond to break is the NO_2-ethylene bond. Mulliken population analysis shows a large positive charge on nitrogen (0.65) and a large negative charge on the nearest carbon, -0.67. The Mayer bond order for this atom is less than one (0.68), indicating a looser interaction as in a regular sp^3 bond.

In a recent study, Mathews et al (Mathews and Ball 2009) analyzed the optimized bond lengths and structures of amino substituted nitroethanes, their equilibrium bond distances were never in excess of 1.7 Å. Kwok have suggested a very fast

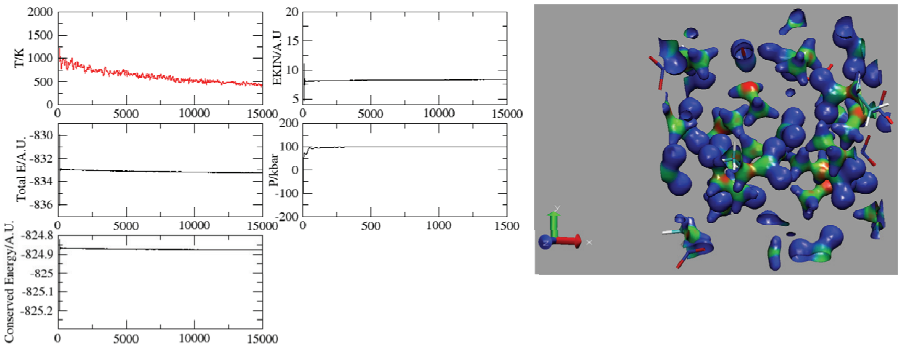

Figure 20: Running average of the larger 15 molecule NVE simulation run (left). Electrostatic potential mapped into the molecular charge density isosurface (0.16 Hartree).

transfer from an exited NO2 to the C-N bond as this was suggested as the primary mechanism as studied from Raman spectra (Kwok, Hung and Phillips 1996). Our results indeed find that even in the initial phases of equilibration, NO_2 bond scission occurs for temperatures of 2000K.

5 Concluding Remarks

Based on known compounds, current theoretical calculations are made to design new possible compounds with desirable properties (Kim, Lee, Hyun, Park, Kwack, Kim, Lee and Lee 2004; Zhang, Shu et al. 2005; Zhang, Liu and Lv 2005). Although up until 2004 results using the Hartree-Fock method were usually reported; this has largely evolved to the uses of larger basis sets and exchange correlation functions within the density functional theory (DFT) formalism. Latter use of molecular dynamics and other atomistic level modeling has shown of use when studying the effects of temperature and defects.

Although the value of the C_{11} constant correlate directly with the experimentally observed sensitivity of the particular systems, (namely TATB > Fox-7 > RDX > b-HM > PETN > NM, TATB, being the most insensitive), prediction of the reactivity and sensitivity of an explosive is complex since it depends on the interaction of mechanical, chemical and thermodynamic conditions. For a perfectly symmetric crystal, compression up to close the initiation pressure showed no signs of mechanical instability. Adiabatic compression showed the largest change in energy for β-HMX. We can correlate this energy requirement with the trend in sensitivity

β-HMX<PETN<NM. Through the calculation of the effect of pressure upon band-gap closing, we can conclude that metallization as the initiation step in an adiabatic uniaxial compression of a perfect crystal can be excluded.

In addition to this, fractures along a given plane can act as energy barriers and hinder a complete reaction, causing unexpected behavior in some cases.

We have studied the [110][001] system in PETN. Γ surface calculations showed interaction in the surface of these grains up to molecular layers. Observed changes in density resulting from the stacking of two grains can have an effect on the detonation pressure. Molecular dynamics simulations have shown the effect of temperature. Constant temperature constant pressure dynamics on large systems have shown a higher number of nitro groups oscillating at the interface. Comparison with other types of systems could provide information about the effect of higher nitro number density in the reactivity and sensitivity to detonation. The observation of the increased stability with respect to applied temperature could indicate the formation of this interface at extreme conditions available through compression or heating. Quenching to lower temperatures would nonetheless render the interface unstable.

Explicit modeling of the electronic degrees of freedom at finite temperatures has emerged as a possibility within the Car-Parrinello method. Here, dynamic behavior at different temperatures that govern the behavior of energetic materials can be studied. Processes like hydrogen bonding, structure evolution and preferential conformations can be easily observed. In our particular case study, fission of the C-NO_2 bond is identified as the initial step of nitroethane thermal decomposition. This is confirmed by Mulliken population analysis.

With regard to novel high energy compounds, multiscale modeling could be applied to the study of nitrogen rich compounds (triazolium salts, and their amino and azido substituted relative compounds) and the effects of the structure. The family of nitrogen rich extended ring systems, triazolim, tetrazolium, by-ciclic salts, utropinium, and tetrazine can be compared. These higher volume salts seem to have increased stability to air, light and a low temperature emission. It has been commonly stated that strain in the molecular structure can be related to the detonation pressure and pressure velocity. Elasticity measurements for these compounds will be of special interest for compounds like cubane and azetidinium based compounds, versus aromatic nitrogen salts, like imidazole based compounds.

Acknowledgement: The research here supported by ARO-MURI: Insensitive Munitions. O.U.O. acknowledges gratefully CONACYT for its kind support for earlier part of his doctoral work. The authors would like to thank the support of the supercomputing centers of Texas A&M College Station and Texas A&M Qatar.

References

(1980): *LASL Explosive Property Data*. Berkley, CA, University of California Press.

Alonso, J., Mañanes, A. (2007): Long-Range van der Waals Interactions in Density Functional Theory. *Theoretical Chemistry Accounts: Theory, Computation, and Modeling (Theoretica Chimica Acta)* 117(4): 467-472.

Antoine, E. D. M. van, der Heijden, Yves, L. M. C., Emanuela Marino, Richard, H. B. Bouma, Gert, J. H. G. Scholtes, Willem Duvalois, Marc, C. P. M. Roelands (2008): Energetic Materials: Crystallization, Characterization and Insensitive Plastic Bonded Explosives. *Propellants, Explosives, Pyrotechnics* 33(1): 25-32.

Bachorz, R. A., Bischoff, F. A., Hofener, S., Klopper, W., Ottiger, P., Leist, R., Frey, J. A., Leutwyler, S. (2008): Scope and limitations of the SCS-MP2 method for stacking and hydrogen bonding interactions. *Physical Chemistry Chemical Physics* 10(19): 2758-2766.

Bacon, G. E., Curry, N. A., Wilson, S. A. (1964): A Crystallographic Study of Solid Benzene by Neutron Diffraction. *Proceedings of the Royal Society of London. Series A, Mathematical and Physical Sciences* 279(1376): 98-110.

Badders, N. R., Wei, C., Aldeeb, A. A., Rogers, W. J., Mannan, M. S. (2006): Predicting the impact sensitivities of polynitro compounds using quantum chemical descriptors. *Journal of Energetic Materials* 24(1): 17-33.

Bagryanskaya, I. Y., Gatilov, Y. V. (1983): Crystal structure of nitromethane. *Journal of Structural Chemistry* 24(1): 150-151.

Bemm, U., Ostmark, H. (1998): 1,1-Diamino-2,2-dinitroethylene: a Novel Energetic Material with Infinite Layers in Two Dimensions. *Acta Crystallographica Section C* 54(12): 1997-1999.

Bilge, M., Kart, H.H., Kart, S. O., Çağın, T. (2009): B3-B1 Phase Transition and Pressure Dependence of the Elastic Properties of ZnS, *Materials Chemistry and Physics* 111, 559-64.

Birch, F. (1947): Finite Elastic Strain of Cubic Crystals. *Physical Review* 71(11): 809.

Birch, F. (1978): Finite strain isotherm and velocities for single-crystal and Polycrystalline NaCl at high pressures and 300/sup 0/K. *J. Geophys. Res. ; Vol/Issue: 83:B3*: Pages: 1257-1268.

BlÖchl, P. E. (1994): Projector augmented-wave method. *Physical Review B* 50(24): 17953.

Boldyreva, E. (2008): High-pressure diffraction studies of molecular organic solids. A personal view. *Acta Crystallographica Section A* 64(1): 218-231.

Boldyreva, E. V. (2003): High-pressure studies of the anisotropy of structural distortion of molecular crystals. *Journal of Molecular Structure* 647(1-3): 159-179.

Booth, A. D., Llewellyn (1947): The crystal structure of pentaerythritol tetranitrate. *J. Chem. Soc.*: 837-846.

Booth, A. D., Llewellyn, F. J. (1947): The Crystal Structure Of Pentaerythritol Tetranitrate. *Journal of the Chemical Society*(JUN): 837-846.

Bouyer, V., Darbord, I., Hervé, P., Baudin, G., Le Gallic, C., Clément, F., Chavent, G. (2006): Shock-to-detonation transition of nitromethane: Time-resolved emission spectroscopy measurements. *Combustion and Flame* 144(1-2): 139-150.

Bower, J. K., Kolb, J. R., Pruneda, C. O. (1980): Polymeric Coatings Effect on Surface Activity and Mechanical Behavior of High Explosives. *Industrial & Engineering Chemistry Product Research and Development* 19(3): 326-329.

Brand, H. V. (2006): Periodic Hartree-Fock study of the elasticity of pentaerythritol tetranitrate. *Chemical Physics Letters* 418(4-6): 428-432.

Brill, T. B., Goetz, F. (1979): Laser Raman Spectra of a-, b-, g-, and d-Octogydro-1, 3,5,7-tetranitro-1,3,5,7,-tetrazocine and Their Temperature Dependence. *The Journal of Chemical Physics* 83(3): 340-346.

Brown, J. M., Slutsky, L. J., Nelson, K. A., Cheng, L.-T. (1988): Velocity of Sound and Equations of State for Methanol and Ethanol in a Diamond-Anvil Cell. *Science* 241(4861): 65-67.

Byrd, E. F. C., Rice, B. M. (2006): Improved prediction of heats of formation of energetic materials using quantum mechanical calculations. *Journal of Physical Chemistry A* 110(3): 1005-1013.

Byrd, E. F. C., Rice, B. M. (2007): Ab Initio Study of Compressed 1,3,5,7-Tetranitro-1,3,5,7-tetraazacyclooctane (HMX), Cyclotrimethylenetrinitramine (RDX), 2,4,6,8,10,12-Hexanitrohexaazaisowurzitane (CL-20), 2,4,6-Trinitro -1,3,5- benzenetriamine (TATB), and Pentaerythritol Tetranitrate (PETN). *J. Phys. Chem. C* 111(6): 2787-2796.

Cady, H. H., Larson, A. C. (1965): The crystal structure of 1,3,5-triamino-2,4,6-trinitrobenzene. *Acta Crystallographica* 18(3): 485-496.

Cady, H. H., Larson, A. C., Cromer, D. T. (1963): The crystal structure of [alpha]-HMX and a refinement of the structure of [beta]-HMX. *Acta Crystallographica* 16(7): 617-623.

Campbell, A. W., Holland, T. E., Malin, M. E., Cotter, T. P. (1956): Detonation Phenomena in Homogeneous Explosives. *Nature* 178(4523): 38-39.

CCSDT (2001): PERYTN11, Cambridg Crystallographic Database.

Chakarova, S. D., Schroder, E. (2005): van der Waals interactions of polycyclic aromatic hydrocarbon dimers. *The Journal of Chemical Physics* 122(5): 054102-054105.

Chakrabarty, A., Çağın, T. (2008): Modeling Mechanical and Thermal Properties of Nanotube Based Nanostructures, *CMC: Computers, Materials & Continua* 3, 167-189.

Chen, C., Wu, J. C. (2001): Correlations between theoretical and experimental determination of heat of formation of certain aromatic nitro compounds. *Computers & Chemistry* 25(2): 117-124.

Choi, S. C., Boutin, H. P. (1970): A study of the crystal structure of b-Cyclotretramethylene tetranitramine by neutron diffraction. *Acta Crystalographica* B26: 1235-1240.

Cobos, C. J. (2005): DFT study of the thermochemistry of gas-phase 1,3,5,7-tetranitro-1,3,5,7-tetraazacyclooctane ([beta]-HMX). *Journal of Molecular Structure: THEOCHEM* 714(2-3): 147-152.

Coleburn, N. L. (1970): Dynamic Bulk Moduli of Several Solids Impacted by Weak Shockwaves. *The Journal of the Acoustical Society of America* 47(1B): 269-272.

Coleburn, N. L., T. P. Liddiard, J. (1966): Hugoniot Equations of State of Several Unreacted Explosives. *The Journal of Chemical Physics* 44(5): 1929-1936.

Cox, E. G. (1958): Crystal Structure of Benzene. *Reviews of Modern Physics* 30(1): 159.

Cromer, D. T., Ryan, R. R., Schiferl, D. (1985): The structure of nitromethane at pressures of 0.3 to 6.0 GPa. *The Journal of Physical Chemistry* 89(11): 2315-2318.

Cromer, D. T. R. R. R., Schiferl, D. (1985): Structure of nitromethane at pressures of 0.3 to 6.0 GPa. *J. Phys. Chem. ; Vol/Issue: 89:11*: Pages: 2315-2318.

Czerski, H., Proud, W. G. (2007): Relationship between the morphology of granular cyclotrimethylene-trinitramine and its shock sensitivity. *Journal of Applied Physics* 102(11): 113515-113518.

Database, C. S. (2007): CCSD, CCSD.

David Rigby, H. S., Eichinger, B. E. (1997): Computer simulations of poly(ethylene oxide): force field, pvt diagram and cyclization behaviour. *Polymer International* 44(3): 311-330.

Day, G. M., Price, S. L., Leslie, M. (2001): Elastic Constant Calculations for Molecular Organic Crystals. *Crystal Growth & Design* 1(1): 13-27.

Dewar, M. J. S., Ritchie, J. P. (1985): Thermolysis of molecules containing NO_2

groups. *Journal of Organic Chemistry* (50): 1031-1036.

Dick, J. J. (1984): Effect of crystal orientation on shock initiation sensitivity of pentaerythritol tetranitrate explosive. *Applied Physics Letters* 44(9): 859-861.

Dick, J. J. (1993): Orientation-dependent explosion sensitivity of solid nitromethane. *J. Phys. Chem.* 97(23): 6193-6196.

Dick, J. J. (1997): Anomalous shock initiation of detonation in pentaerythritol tetranitrate crystals. *Journal of Applied Physics* 81(2): 601-612.

Dlott, D. D., Peter, P., Jane, S. M. (2003): Chapter 6 Fast molecular processes in energetic materials. *Theoretical and Computational Chemistry*, Elsevier. **Volume 13:** 125-191.

Dovesi, R., Saunders, V. R., Roetti, C., Orlando, R., Zicovich-Wilson, C. M., Pascale, F., Civalleri, B., Doll, K., Harrison, N. M., Bush, I. J., Ph., D. A., Llunell, M. (2007): Crystal06, `www.crystal.unito.it`.

Drake, G. W., Hawkins, T. W., Hall, L. A., Boatz, J. A., Brand, A. J. (2005): Structural and theoretical investigations of 3,4,5-triamino-1,2,4-triazolium salts. *Propellants Explosives Pyrotechnics* 30(5): 329-337.

Edwards, J., Eybl, C., Johnson, B. (2004): Correlation between sensitivity and approximated heats of detonation of several nitroamines using quantum mechanical methods. *International Journal of Quantum Chemistry* 100(5): 713-719.

Engel, E. (2003): Orbital-dependent functionals for the exchange-correlation energy: a third generation of density functionals. *A primer inf Density Functional Theory*. C. Fiolhais, F. Nogueira and M. Marques. Berlin, Springer.

Evers, J., Klapotke, T. M., Mayer, P., Oehlinger, G., Welch, J. (2006): α- and β-FOX-7, Polymorphs of a High Energy Density Material, Studied by X-ray Single Crystal and Powder Investigations in the Temperature Range from 200 to 423 K. *Inorganic Chemistry* 45(13): 4996-5007.

Firsich, D. W. (1984): Energetic Materials Separation and specific polymorph preparations via thermal gradient sublimation. *Journal of Hazardous Materials* 9: 133-137.

Fischer, G., Zarembow.J (1970): Elastic properties of urea monocrystals. *Comptes Rendus Hebdomadaires Des Seances De L Academie Des Sciences Serie B* 270(13): 852-&.

Gallagher, H. G., Halfpenny, P. J., Miller, J. C., Sherwood, J. N. and Tabor, D. (1992): Dislocation Slip Systems in Pentaerythritol Tetranitrate (PETN) and Cyclotrimethylene Trinitramine (RDX) [and Discussion]. *Philosophical Transactions: Physical Sciences and Engineering* 339(1654): 293-303.

Gatti, C., Saunders, V. R., Roetti, C. (1994): Crystal field effects on the topolog-

ical properties of the electron density in molecular crystals: The case of urea. *The Journal of Chemical Physics* 101(12): 10686-10696.

Gibbs, T. R., Popolato, A., Baytos, J. F. (1980): *LASL explosive property data*. Berkeley CA., University of California Press

Gilardi, R. D., George, C. F. (1984): CIWMAW. *Cambridge Structural Database*, The Cambridge Crystallographic Data Centre.

Golovina, N. I., Titkov, A. N., Raevskii, A. V., Atovmyan, L. O. (1994): Kinetics and Mechanism of Phase Transitions in the Crystals of 2,4,6-Trinitrotoluene and Benzotrifuroxane. *Journal of Solid State Chemistry* 113(2): 229-238.

Gonzalez, C., Lim, E. C. (2003): Evaluation of the Hartree-Fock Dispersion (HFD) Model as a Practical Tool for Probing Intermolecular Potentials of Small Aromatic Clusters: Comparison of the HFD and MP2 Intermolecular Potentials. *J. Phys. Chem. A* 107(47): 10105-10110.

Goursot, A., Mineva, T., Kevorkyants, R., Talbi, D. (2007): Interaction between n-Alkane Chains: Applicability of the Empirically Corrected Density Functional Theory for Van der Waals Complexes. *J. Chem. Theory Comput.* 3(3): 755-763.

Grimme, S., Antony, J., Schwabe, T., Muck-Lichtenfeld, C. (2007): Density functional theory with dispersion corrections for supramolecular structures, aggregates, and complexes of (bio)organic molecules. *Organic & Biomolecular Chemistry* 5(5): 741-758.

Gruzdkov, Y. A., Dreger, Z. A., Gupta, Y. M. (2004): Experimental and Theoretical Study of Pentaerythritol Tetranitrate Conformers. *The Journal of Physical Chemistry A* 108(29): 6216-6221.

Hagler, A. T., Dauber, P., Lifson, S. (1979): Consistent force field studies of intermolecular forces in hydrogen-bonded crystals. 3. The C:OH-O hydrogen bond and the analysis of the energetics and packing of carboxylic acids. *Journal of the American Chemical Society* 101(18): 5131-5141.

Hagler, A. T., Huler, E., Lifson, S. (1974): Energy functions for peptides and proteins. I. Derivation of a consistent force field including the hydrogen bond from amide crystals. *J. Am. Chem. Soc.* 96(17): 5319-5327.

Hagler, A. T., Lifson, S. (1974): Energy functions for peptides and proteins. II. Amide hydrogen bond and calculation of amide crystal properties. *Journal of the American Chemical Society* 96(17): 5327-5335.

Hagler, A. T., Lifson, S., Dauber, P. (1979): Consistent force field studies of intermolecular forces in hydrogen-bonded crystals. 2. A benchmark for the objective comparison of alternative force fields. *Journal of the American Chemical Society* 101(18): 5122-5130.

Halgren, T. A. (1992): The representation of van der Waals (vdW) interactions in molecular mechanics force fields: potential form, combination rules, and vdW parameters. *J. Am. Chem. Soc.* 114(20): 7827-7843.

Hartmut Kröber, U. T. (2008): Crystallization of Insensitive HMX. *Propellants, Explosives, Pyrotechnics* 33(1): 33-36.

Haussuhl, S. (2001): Elastic and thermoelastic properties of selected organic crystals: acenaphthene, trans-azobenzene, benzophenone, tolane, trans-stilbene, dibenzyl, diphenyl sulfone, 2,2 '-biphenol, urea, melamine, hexogen, succinimide, pentaerythritol, urotropine, malonic acid, dimethyl malonic acid, maleic acid, hippuric acid, aluminium acetylacetonate, iron acetylacetonate, and tetraphenyl silicon. *Zeitschrift Fur Kristallographie* 216(6): 339-353.

Hemmi, N., Dreger, Z. A., Gruzdkov, Y. A., Winey, J. M., Gupta, Y. M. (2006): Raman Spectra of Shock Compressed Pentaerythritol Tetranitrate Single Crystals: Anisotropic Response. *J. Phys. Chem. B* 110(42): 20948-20953.

Hepburn, J., Scoles, G., Penco, R. (1975): A simple but reliable method for the prediction of intermolecular potentials. *Chemical Physics Letters* 36(4): 451-456.

Hu, W.-F., He, T.-J., Chen, D.-M. (Liu, Fan-Chen): Theoretycak stuyd of the CH_3NO_2 unimolecular decomposition potential energy surfaces. *Journal of Physical Chemistry A* 106(32): 7294-7303.

Jeffrey, G. A., Ruble, J. R., McMullan, R. K., Pople, J. A. (1987): The Crystal Structure of Deuterated Benzene. *Proceedings of the Royal Society of London. Series A, Mathematical and Physical Sciences* 414(1846): 47-57.

John R. Kolb, H. F. R. (1979): Growth of 1,3,5-Triamino-2,4,6-trinitrobenzene (TATB) I. Anisotropic thermal expansion. *Propellants, Explosives, Pyrotechnics* 4(1): 10-16.

Ju, X. H., Xu, X. J., Xiao, H. M. (2005): Computational study of picric acid and potassium picrate. *Journal of Energetic Materials* 23(2): 121-130.

Kalay, M., Kart, H. H., Kart, S. O., Çağın, T. (2009): Structural parameters, elastic constants and transition pressures of ZnO from first-principle calculations, *J. Alloy. Comp.* 484, 431-438

Kart, S. O., Uludogan, M., Karaman, I., Çağın, T. (2008): DFT Studies on Structure, Mechanics and Phase Behavior of Magnetic Shape Memory Alloys: Ni2MnGa *Phys. Stat. Sol.* (a) 205, 1026-35

Kim, C. K., Lee, K. A., Hyun, K. H., Park, H. J., Kwack, I. Y., Kim, C. K., Lee, H. W., Lee, B. S. (2004): Prediction of physicochemical properties of organic molecules using van der Waals surface electrostatic potentials. *Journal of Computational Chemistry* 25(16): 2073-2079.

Kitson, D. H., Hagler, A. T. (1988): Catalysis of a rotational transition in a peptide by crystal forces. *Biochemistry* 27(19): 7176-7180.

Kitson, D. H., Hagler, A. T. (1988): Theoretical studies of the structure and molecular dynamics of a peptide crystal. *Biochemistry* 27(14): 5246-5257.

Kleis, J., Schroder, E. (2005): van der Waals interaction of simple, parallel polymers. *The Journal of Chemical Physics* 122(16): 164902-164907.

Kohn, W., Sham, L. J. (1965): Self-Consistent Equations Including Exchange and Correlation Effects. *Physical Review* 140(4A): A1133.

Korolev, V. L., Petukhova, T. V., Pivina, T. S., Sheremetev, A. B., Miroshnichenko, E. A., Ivshin, V. P. (2004): Studies on the structure and thermochemical properties of nitro- and nitrosopipecazines by the methods of quantum chemistry. *Khimiya Geterotsiklicheskikh Soedinenii*(12): 1817-1839.

Kresse, G., Furthmüller, J. (1996): Efficiency of ab-initio total energy calculations for metals and semiconductors using a plane-wave basis set. *Computational Materials Science* 6(1): 15-50.

Kresse, G., Furthmüller, J. (1996): Efficient iterative schemes for ab initio total-energy calculations using a plane-wave basis set. *Physical Review B* 54(16): 11169.

Kresse, G., Hafner, J. (1993): Ab initio molecular dynamics for liquid metals. *Physical Review B* 47(1): 558.

Kresse, G., Hafner, J. (1994): Norm-conserving and ultrasoft pseudopotentials for first-row and transition elements. *Journal of Physics: Condensed Matter*(40): 8245.

Kresse, G., Joubert, D. (1999): From ultrasoft pseudopotentials to the projector augmented-wave method. *Physical Review B* 59(3): 1758.

Kunz, B. A. (1995): *An Ab Initio Investigation of Crystalline PETN*. Decomposition, Combustion, and Detonation Chemistry of Energetic Materials, Boston, Materials Research Society.

Kurita, N., Inoue, H., Sekino, H. (2003): Adjustment of Perdew-Wang exchange functional for describing van der Waals and DNA base-stacking interactions. *Chemical Physics Letters* 370(1-2): 161-169.

Kwok, W. M., Hung, M. S., Phillips, D. L. (1996): Femtosecond photodissociation dynamics of nitroethane and 1-nitropropane in the gas and solution phases from resonance Raman intensity analysis. *Molecular Physics*, Taylor & Francis Ltd. 88: 517-531.

Landerville, A. C., Oleynik, I. I., White, C. T. (2009): Reactive Molecular Dynamics of Hypervelocity Collisions of PETN Molecules. *The Journal of Physical Chemistry A* 113(44): 12094-12104.

LeSar, R. (1984): Electron-gas plus damped-dispersion model for intermolecular forces. The rare-gas and hydrogen-helium, hydrogen-neon, and hydrogen-argon potentials. *J. Phys. Chem.* 88(19): 4272-4278.

Lewis L. Stevens, N. V., Daniel E. Hooks, Dana M. Dattelbaum, (2008): Hydrostatic Compression Curve for Triamino-Trinitrobenzene Determined to 13.0 GPa with Powder X-Ray Diffraction. *Propellants, Explosives, Pyrotechnics* 33(4): 286-295.

Li, J. S., Huang, Y. G., Dong, H. S. (2005): A theoretical study of polynitropyridines and their N-oxides. *Journal of Energetic Materials* 23(3): 133-149.

Lifson, S., Hagler, A. T., Dauber, P. (1979): Consistent force field studies of intermolecular forces in hydrogen-bonded crystals. 1. Carboxylic acids, amides, and the C:O.cntdot..cntdot..cntdot.H- hydrogen bonds. *Journal of the American Chemical Society* 101(18): 5111-5121.

Lionel Borne, J.-C. P., Christian Spyckerelle, (1999): Quantitative Characterization of Internal Defects in RDX Crystals. *Propellants, Explosives, Pyrotechnics* 24(4): 255-259.

Lozano, A., Fernandez, J. (2007): Surface hardening of railway crossings comprises high frequency generation and sonic impacting prior to explosion on hardened surface. *ES2275366*. P. O. European. Spain, Corral, Bescos M. ES2275366: 7.

Lyman, J. L., Liau, Y.-C., Brand, H. V. (2002): Thermochemical functions for gas-phase, 1,3,5,7-tetranitro-1,3,5,7-tetraazacyclooctane (HMX), its condensed phases, and its larger reaction products. *Combustion and Flame* 130(3): 185-203.

Maharrey, S., Behrens, R. (2005): Thermal decomposition of energetic materials. 5. Reaction processes of 1,3,5-trinitrohexahydro-s-triazine below its melting point. *Journal of Physical Chemistry A* 109(49): 11236-11249.

Main, P. (1985): Structure of the fourth form of 1,3,5,7-tetraazacyclooctane (g-hmx), 2C4,H8,N8,O8*0.5H2O. *Acta Crystalographica* C41(1351-1354):

Manaa, M. R., Fried, L. E. (1998): DFT and ab Initio Study of the Unimolecular Decomposition of the Lowest Singlet and Triplet States of Nitromethane. *The Journal of Physical Chemistry A* 102(48): 9884-9889.

Manaa, M. R., Reed, E. J., Fried, L. E., Goldman, N. (2009): Nitrogen-Rich Heterocycles as Reactivity Retardants in Shocked Insensitive Explosives. *Journal of the American Chemical Society* 131(15): 5483-5487.

Marcus, E., Pavel, H., Thomas, F., Sandor, S., Efthimios, K. (2001): Hydrogen bonding and stacking interactions of nucleic acid base pairs: A density-functional-theory based treatment. *The Journal of Chemical Physics* 114(12): 5149-5155.

Mathews, K. Y., Ball, D. W. (2009): Computational study of the structures and properties of aminonitroethane molecules. *Journal of Molecular Structure: THEOCHEM* 902(1-3): 15-20.

Mayo, S. L., Olafson, B. D., Goddard, W. A. (1988): DREDING: A generic force field for molecular simulations *Journal of Physical Chemistry* 94: 8897-8909.

McClellan, J. J., Hughes, T. F., Bartlett, R. J. (2005): Application of the transfer Hamiltonian formalism to high-energy model systems. *International Journal of Quantum Chemistry* 105(6): 914-920.

McKean, D. C., Watt, R. A. (1976): Vibrational spectra of nitromethanes and the effects of internal rotation. *Journal of Molecular Spectroscopy* 61(2): 184-202.

McKee, M. L. (1986): Ab initio study of rearrangements on the nitromethane potential energy surfacec. *Journal of the American Chemical Society* 108(19): 5784-5792.

Meents, A., Dittrich, B., Johnas, S. K. J., Thome, V., Weckert, E. F. (2008): Charge-density studies of energetic materials: CL-20 and FOX-7. *Acta Crystallographica Section B* 64(1): 42-49.

Meents, A., Dittrich, B., Johnas, S. K. J., Thome, V., Weckert, E. F. (2008): Charge-density studies of energetic materials: CL-20 and FOX-7. Corrigendum. *Acta Crystallographica Section B* 64(4): 519.

Miller, M. S. (1995): *Three-phase combustion modelling: frozen ozone, a prototype system*. Decomposition, Combustion, and Detonation Chemistry of Energetic Materials, Boston, Materials Research Society.

Moore, D. S., Funk, D. J., McGrane, S. D. (2005): At the confluence of experiment and simulation: Ultrafast laser spectroscopic studies of shock compressed energetic materials. *Chemistry at Extreme Conditions*: 369-397.

Nguyen, M. T., Le, H. T., Hajgato, B., Veszpremi, T., Lin, M. C. (2003): Nitromethanemethyl nitrite rearrangement: a perisisten discrepancy between theory and experiment. *Journal of Physical Chemistry A* 107(21): 4286-4291.

Novozhilov, B. V. (2005): Combustion of energetic materials in an acoustic field (review). *Combustion Explosion and Shock Waves* 41(6): 709-726.

Olinger, B., Cady, H. H. (1976): *The hydrostatic compression of explosives and detonation products to 10 GPa (100 kbars) and their calculated shock compression: results for PETN, TATB, CO_2 and H_2O*. Sixth symposium on detonation, Coronado, California, Office of naval reasearch.

Olinger, B., Halleck, P. M., Cady, H. H. (1975): The isothermal linear and volume compression of pentaerythritol tetranitrate (PETN) to 10 GPa (100 kbar) and the calculated shock compression. *The Journal of Chemical Physics* 62(11): 4480-

4483.

Ortmann, F., Bechstedt, F., Schmidt, W. G. (2006): Semiempirical van der Waals correction to the density functional description of solids and molecular structures. *Physical Review B (Condensed Matter and Materials Physics)* 73(20): 205101-205110.

Ouillon, R., Pinan-Lucarre, J. P., Ranson, P., Baranovic, G. (2002): Low-temperature Raman spectra of nitromethane single crystals. Lattice dynamics and Davydov splittings. *The Journal of Chemical Physics* 116(11): 4611-4625.

Palmer, S. J. P., Field, J. E. (1982): The deformation and fracture of b-HMX. *Proc. R. Soc. London, Ser. A* 383: 399-407.

Pascale, F., Zicovich-Wilson, C. M., López Gejo, F., Civalleri, B., Orlando, R., Dovesi, R. (2004): The calculation of the vibrational frequencies of crystalline compounds and its implementation in the CRYSTAL code. *Journal of Computational Chemistry* 25(6): 888-897.

Patterson, J. E., Lagutchev, A. S., Hambir, S. A., Huang, W., Yu, H. and Dlott, D. D. (2005): Time- and space-resolved studies of shock compression molecular dynamics. *Shock Waves* 14(5-6): 391-402.

Perdew, J. P., Burke, K., Ernzerhof, M. (1996): Generalized Gradient Approximation Made Simple. *Physical Review Letters* 77(18): 3865.

Perger, W. F., Pandey, R., Blanco, A. M., Zhao, J. (2004): First-Principles intermolecular binding energies in organic molecular crystals. *Elsevier Science*. Amsterdam, Netherlands: 12.

Pham, H. H., Çağın, T. (2010) Lattice Dynamics and second and third order elastic constants of Iron at elevated pressures. *CMC: Computers, Materials & Continua*, this issue.

Pinkerton, A. A., Martin, A. (1995): *Charge densities and electrostatic potentials for energetic materials*. Decomposition, Combustion, and Detonation Chemistry of Energetic Materials, Boston, Materials Research Society.

Plimpton, S. (1995): Fast Parallel Algorithms for Short-Range Molecular Dynamics. *Journal of Computational Physics* 117: 1-19.

Pnina Dauber-Osguthorpe, V. A. R., David J. Osguthorpe, Jon Wolff, Moniqe Genest, Arnold T. Hagler, (1988): Structure and energetics of ligand binding to proteins: *Escherichia coli* dihydrofolate reductase-trimethoprim, a drug-receptor system. *Proteins: Structure, Function, and Genetics* 4(1): 31-47.

Pople, J. A., von Rague Schleyer, P., Kaneti, J., Spitznagel, G. W. (1988): Accurate theoretical estimates of the electron affinities of AHn molecules by isogyric comparisons. Proton affinities of AHn- anions. *Chemical Physics Letters* 145(5):

359-364.

Qin Wu, H. O., Weitao, Y. (2003): Algebraic Equation And Iterative Optimization For The Optimized Effective Potential In Density Functional Theory. *Journal of Theoretical & Computational Chemistry* 2(4): 627-638.

Qiu, L., Xiao, H. M., Ju, X. H., Gong, X. D. (2005): Theoretical study of the structures and properties of cyclic nitramines: Tetranitrotetraazadecalin (TNAD) and its isomers. *International Journal of Quantum Chemistry* 105(1): 48-56.

Rappe, A. K., Casewit, C. J., Colwell, K. S., Goddard, W. A., Skiff, W. M. (1992): UFF, a full periodic table force field for molecular mechanics and molecular dynamics simulations. *Journal of the American Chemical Society* 114(25): 10024-10035.

Rappe, A. K., Goddard, W. A. (1991): Charge equilibration for molecular dynamics simulations. *The Journal of Physical Chemistry* 95(8): 3358-3363.

Ruth M. Doherty, Duncan S. W. (2008): Relationship Between RDX Properties and Sensitivity. *Propellants, Explosives, Pyrotechnics* 33(1): 4-13.

Sevik, C., Çağın, T. (2009): Structure and electronic properties of CeO_2, ThO_2 and their alloys, Phys. Rev B. 80, 014108

Sewell, T. D., Menikoff, R., Bedrov, D., Smith, G. D. (2003): A molecular dynamics simulation study of elastic properties of HMX. *The Journal of Chemical Physics* 119(14): 7417-7426.

Slater, J. C., Kirkwood, J. G. (1931): The Van der Waalls forces in gases. *Physical Review* 37: 682-697.

Son, S. F., Asay, B. W., Bdzil, J. B., Kober, E. M. (1995): *Reaction Rate Modeling in the deflagration to detonation transition of granualr energetic materials*. Decomposition, Combustion, and Detonation Chemistry of Energetic Materials, Boston, Materials Research Society.

Sorescu, D. C., Rice, B. M., Thompson, D. L. (1999): Theoretical Studies of the Hydrostatic Compression of RDX, HMX, HNIW, and PETN Crystals. *The Journal of Physical Chemistry B* 103(32): 6783-6790.

Sorescu, D. C., Rice, B. M., Thompson, D. L. (2000): Theoretical Studies of Solid Nitromethane. *J. Phys. Chem. B* 104(35): 8406-8419.

Soto, M. R. (1995): *A theoretical study of BF+OH and BO+HF reactions*. Decomposition, Combustion, and Detonation Chemistry of Energetic Materials, Boston, Materials Research Society.

Soulard, L. (1995): *Molecular dynamics calculations on the properties of the reaction zone in the liquid explosive*. Decomposition, Combustion, and Detonation Chemistry of Energetic Materials, Boston, Materials Research Society.

Srivathsa, B., Ramakrishnan, N. (2008): An analytical model for explosive compaction of powder to cylindrical billets through axial detonation. *Computers, Materials and Continua,* 7(1): 9-23.

Stevens, L. L., Eckhardt, C. J. (2005): The elastic constants and related properties of beta-HMX determined by Brillouin scattering. *The Journal of Chemical Physics* 122(17): 174701-174708.

Stevens, L. L., Velisavljevic, N., Hooks, D. E., Dattelbaum, D. M. (2008): The high-pressure phase behavior and compressibility of 2,4,6-trinitrotoluene. *Applied Physics Letters* 93(8): 081912-081913.

Sun, B., Winey, J. M., Hemmi, N., Dreger, Z. A., Zimmerman, K. A., Gupta, Y. M., Torchinsky, D. H., Nelson, K. A. (2008): Second-order elastic constants of pentaerythritol tetranitrate and cyclotrimethylene trinitramine using impulsive stimulated thermal scattering. *Journal of Applied Physics* 104(7): 073517-073516.

Sun, D. W., Garimella, S. V., Singh, S., Naik, N. (2005): Numerical and experimental investigation of the melt casting of explosives. *Propellants Explosives Pyrotechnics* 30(5): 369-380.

Sun, H. (1998): COMPASS: An ab Initio Force-Field Optimized for Condensed-Phase Applications Overview with Details on Alkane and Benzene Compounds. *The Journal of Physical Chemistry B* 102(38): 7338-7364.

Sun, H., Ren, P., Fried, J. R. (1998): The COMPASS force field: parameterization and validation for phosphazenes. *Computational and Theoretical Polymer Science* 8: 229-246.

Sun, H., Rigby, D. (1997): Polysiloxanes: ab initio force field and structural, conformational and thermophysical properties. *Spectrochimica Acta Part A: Molecular and Biomolecular Spectroscopy* 53(8): 1301-1323.

Suzuki, S., Green, P. G., Bumgarner, R. E., Dasgupta, S., Goddard, W. A., III and Blake, G. A. (1992): Benzene Forms Hydrogen Bonds with Water. *Science* 257(5072): 942-945.

Swaminathan, S., Craven, B. M., McMullan, R. K. (1984): The crystal structure and molecular thermal motion of urea at 12, 60 and 123 K from neutron diffraction. *Acta Crystallographica Section B* 40(3): 300-306.

Tao, J., Perdew, J. P. (2005): Test of a nonempirical density functional: Short-range part of the van der Waals interaction in rare-gas dimers. *The Journal of Chemical Physics* 122(11): 114102-114107.

Tarasov, M., Karpenko, I., Sudovtsov, V., Tolshmyakov, A. (2007): Measuring the brightness temperature of a detonation front in a porous explosive. *Combustion, Explosion, and Shock Waves* 43(4): 465-467.

Terao, K. (2007): *Irreversible phenomena : ignitions, combustion, and detonation waves*. Berlin; New York, Springer.

Thonhauser, T., Cooper, V. R., Shen, L., Puzder, A., Hyldgaard, P. and Langreth, D. C. (2007): Van der Waals density functional: Self-consistent potential and the nature of the van der Waals bond. *cond-mat/0703442*.

Tokmakoff, A., Fayer, M. D., Dlott, D. D. (1993): Chemical reaction initiation and hot-spot formation in shocked energetic molecular materials. *The Journal of Physical Chemistry* 97(9): 1901-1913.

Trevino, S. F., Prince, E., Hubbard, C. R. (1980): Refinement of the structure of solid nitromethane. *The Journal of Chemical Physics* 73(6): 2996-3000.

Trotter, J., Williston, C. S. (1966): Bond lengths and thermal vibrations in m-dinitrobenzene. *Acta Crystallographica* 21(2): 285-288.

Troullier, N., Martins, J. L. (1991): Efficient pseudopotentials for plane-wave calculations. *Physical Review B* 43(3): 1993.

Tsai, D. H. (1995): *Hot spots in a molecular solid under rapid compression: energy sharing among the T-R-V degrees of freedom*. Decomposition, Combustion, and Detonation Chemistry of Energetic Materials, Boston, Materials Research Society.

Tsuzuki, S., Luthi, H. P. (2001): Interaction energies of van der Waals and hydrogen bonded systems calculated using density functional theory: Assessing the PW91 model. *The Journal of Chemical Physics* 114(9): 3949-3957.

Ugliengo, P. (2006): MOLDRAW: A Program to Display and Manipulate Molecular and Crystal Structures. Torino.

Ugliengo, P., Viterbo, D., Chiari, G. (1993): MOLDRAW - Molecular Graphics On A Personal-Computer. *Zeitschrift Fur Kristallographie* 207: 9-23.

Uludogan, M., Çağın, T., Goddard W.A. (2006): First Principles Approach to $BaTiO_3$ Turk. J. Phys. 30, 277-285.

Uludogan, M., Guarin, D.P., Gomez, Z. E., Çağın, T., Goddard W.A. (2008): DFT studies on ferroelectric ceramics and their alloys *CMES: Computer Modeling in Engineering and Sciences*, Vol. 24, 215-38

Urtiew, P. A., Tarver, C. M. (2005): Shock initiation of energetic materials at different initial temperatures (review): *Combustion Explosion and Shock Waves* 41(6): 766-776.

Volker Weiser, S. K., Norbert Eisenreich, (2001): Influence of the Metal Particle Size on the Ignition of Energetic Materials. *Propellants, Explosives, Pyrotechnics* 26(6): 284-289.

White, C. T., Barrett, J. J. C., Mintmire, J. W., Elert, M. L. (1995): *Effects of nanoscale voids on the sensitivity of model energetic materials*. Decomposition, Combustion, and Detonation Chemistry of Energetic Materials, Boston, Materials Research Society.

Williams, R. W., Malhotra, D. (2006): van der Waals corrections to density functional theory calculations: Methane, ethane, ethylene, benzene, formaldehyde, ammonia, water, PBE, and CPMD. *Chemical Physics* 327(1): 54-62.

Winey, J. M., Gupta, Y. M. (2001): Second-order elastic constants for pentaerythritol tetranitrate single crystals. *Journal of Applied Physics* 90(3): 1669-1671.

Wojcik, G., Mossakowska, I., Holband, J., Bartkowiak, W. (2002): Atomic thermal motions studied by variable-temperature X-ray diffraction and related to non-linear optical properties of crystalline meta-di-nitrobenzene. *Acta Crystallographica Section B* 58(6): 998-1004.

Wu, X., Vargas, M. C., Nayak, S., Lotrich, V., Scoles, G. (2001): Towards extending the applicability of density functional theory to weakly bound systems. *The Journal of Chemical Physics* 115(19): 8748-8757.

Xiao, H. M., Ju, X. H., Xu, L. N., Fang, G. Y. (2004): A density-functional theory investigation of 3-nitro-1,2,4-triazole-5-one dimers and crystal. *Journal of Chemical Physics* 121(24): 12523-12531.

Xu, X., Goddard, W. A., III (2004): From The Cover: The X3LYP extended density functional for accurate descriptions of nonbond interactions, spin states, and thermochemical properties. *PNAS* 101(9): 2673-2677.

Yoo, C.-S., Cynn, H. (1999): Equation of state, phase transition, decomposition of beta-HMX (octahydro-1,3,5,7-tetranitro-1,3,5,7-tetrazocine) at high pressures. *The Journal of Chemical Physics* 111(22): 10229-10235.

Zel'dovich, Y. B., Raizer, Y. P. (2001): *Physics of shock waves and high-temperature hydrodynamic phenomena*. Mineola, N.Y., Dover Publications.

Zeman, S. (2007): Sensitivities of High Energy Compounds. *High Energy Density Materials*: 195-271.

Zepeda-Ruiz, L. A., Maiti, A., Gee, R., Gilmer, G. H., Weeks, B. L. (2006): Size and habit evolution of PETN crystals–a lattice Monte Carlo study. *Journal of Crystal Growth* 291(2): 461-467.

Zhang, C. Y., Shu, Y. J., Zhao, X. D., Dong, H. S., Wang, X. F. (2005): Computational investigation on HEDM of azoic and azoxy derivatives of DAF, FOX-7, TATB, ANPZ and LLM-105. *Journal of Molecular Structure-Theochem* 728(1-3): 129-134.

Zhang, Y. X., Liu, D. B., Lv, C. X. (2005): Preparation and characterization of

reticular nano-HMX. *Propellants Explosives Pyrotechnics* 30(6): 438-441.

Zhao, Q. H., Zhang, S. W., Li, Q. S. (2005): A direct ab initio dynamics study of the initial decomposition steps of gas phase 1,3,3-trinitroazetidine. *Chemical Physics Letters* 412(4-6): 317-321.

Zicovich-Wilson, C. M., Dovesi, R., Saunders, V. R. (2001): A general method to obtain well localized Wannier functions for composite energy bands in linear combination of atomic orbital periodic calculations. *The Journal of Chemical Physics* 115(21): 9708-9719.

Zicovich-Wilson, C. M., Pascale, F., Roetti, C., Saunders, V. R., Orlando, R., Dovesi, R. (2004): Calculation of the vibration frequencies of crystalline compounds and its implementation in the crystal code. *Journal of Computational Chemistry* 25: 888-897.